Technical Report

DYNAMIC RESPONSE OF PRESSURE TRANSMISSION LINES TO PULSE INPUT

by

Arpad Gorove and J. E. Cermak

U. S. Army Research Grant
DA-AMC-28-043-65-G20

Fluid Dynamics and Diffusion Laboratory
College of Engineering
Colorado State University
Fort Collins, Colorado

June 1967

CER66-67AP-JEC51

ABSTRACT

DYNAMIC RESPONSE OF PRESSURE TRANSMISSION LINES TO PULSE INPUT

The dynamic response of pressure transmission lines to pulse input was investigated experimentally. The most commonly used commercially available flexible Tygon tubings were examined at a constant 1/2-psi air pressure with a frequency up to 300 cps. Short tubings, from 1 inch to 3 feet and inside diameters between .052 inch and 1/4 inch, were tested in the experiment. Pressure transducers were selected which had very small internal volume and the reference transducer was kept at a practical minimum distance from the pressure source. Tubing with and without inlet restriction has been investigated to determine the phenomenon of resonant frequency. To determine the effect of the elastic wall of the tubing on the pressure response, comparison measurements were taken in rigid wall, flexible Tygon, and rubber tubings. Phase shift of flexible tubings with various lengths and inside diameters were determined for the frequency range 0-300 cps.

TABLE OF CONTENTS

LIST OF FIGURES

LIST OF FIGURES - continued

LIST OF FIGURES - continued

LIST OF SYMBOLS

Symbol	Definition	Dimension*
A	tube area	L^2
c	velocity of sound	LT^{-1}
d	inside diameter of tube	L
E_c	elastic modulus of tube	$ML^{-1}T^{-2}$
f	frequency	T^{-1}
f_r	resonant frequency	T^{-1}
h	wall thickness of tube	L
ℓ	length of tube	L
M	mass flow	MT^{-1}
Q	volumetric flow	L^3T^{-1}
P	pressure	$ML^{-1}T^{-2}$
t	time	T
u	velocity in x direction	LT^{-1}
V	volume of pressure sensing instrument	L^3
x	distance along the passage from its entrance	L
α	attenuation constant	---
β	propagation constant	---
ξ	damping ratio	---
κ	specific heat	LT^{-1}

* L = length, M = mass, T = time

LIST OF SYMBOLS - continued

Symbol	Definition	Dimension
λ	wave length	L
μ	fluid viscosity	ML^{-1}-T^{-1}
ν	Poissons ratio	---
ρ	fluid density	ML^{-3}
ω_n	natural frequency	T^{-1}

Subscripts

1	state in reference/atmospheric condition/
2	state in the inlet of tube
3	state in the P.T. end of tube
4	state in the P.T. volume
r	state in the restriction

Chapter I

INTRODUCTION

In many research and industrial processes it is necessary to know or to utilize the pressure at one or more points in a fluid conduit. It is not always possible to place an instrument directly into the conduit at those points. In the low pressure transducer, the pressure-sensitive diaphragm is usually made large to increase the output per unit pressure because of the requirement to measure small pressure changes. It is quite difficult or impossible to arrange for the diaphragm to be flush with the surface of the space in which the pressure changes take place. In consequence, the use of the pressure transmission lines seems to be unavoidably necessary. It is desirable to use flexible lines especially in research applicatons. Flexible tubings are made of elastic materials, often with very thin wall; therefore, the tubing may show elastic properties. Thus, two types of pressure lines enter into the problem of defining their response characteristics: rigid wall with constant cross section and elastic wall with external constraints. In dynamic pressure measurements, the evaluation of response characteristics of connecting systems is required. Before 1950, the only solution for the dynamic response of pressure lines was generally based on an elementary theory that considers the system as equivalent to an R-C electrical network (15, 20). The main defect of this theory is that it does not provide criteria for the limits of its applicability. The paper by A. S. Iberall (8) provides the first

complete theoretical solution for response of pressure lines (rigid wall). At present, Iberall's mathematical treatment of the problem is the most rigorous and has the best ability to solve the line response problem.

Several experiments have been undertaken in order to study the pressure transmission line response. Some of the experimental data, as mentioned in Refs.(16) and (17), have been compared to Iberall's theoretical calculations. The reported comparisons between Iberall's theory and experiment have been quite poor. It was presumed that Iberall's theory was considerably more accurate than these experiments indicate. The possible reasons for the poor results of the comparison can be summarized as follows:

1. Iberall's theory can be applied only to non-turbulent flow, i.e., Reynolds number less than 2000.
2. With large lines, considerable distortion of the input signal is caused near the line resonant frequencies. This distortion causes considerable difficulty when measuring the amplitude of input signal.
3. Iberall's equations are valid for an infinite volume at the input end of the line. Because line resonance implies reflected waves in the transmission line, the boundary conditions at the input end, and therefore the response, depend upon the input volume.
4. The pneumatic pressure transmitter has a pneumatic feedback-loop with broad resonant peak. The feedback-loop will, therefore, interact with the reflected signals from the line and change the line response.

5. The graphs which Iberall presented in his paper in order to simplify the solution of the problem will cause some deviation because of reading and interpolation errors.

Iberall's equations are sufficiently complicated so that they have not had wide use. In order to obtain a reliable comparison between the derived equations and experimentally obtained data, an I.B.M. computer program has been devised which calculates the system behavior using Iberall's equations. Only the exact version of his equations was used in the computer program to avoid any possible error during calculations (computer program generates answers accurate to better than .1%)(16). Laboratory experiments (17) were conducted using condenser microphones to measure the response of tubings of different diameter, containing atmospheric air. The experimental and calculated results agreed within experimental accuracy for intermediate length of tubing (4 to 8 ft). Considerable errors were found, however, when shorter tubings were used.

The second type pressure line, the elastic one, is discussed in Ref. (21) and is related to the blood flow theory.

According to Refs.(4, 8, 16, 17) the experimental results of the behavior of rigid pressure transmission lines follow closely the theoretical predictions from a length approximately 4 ft and longer. Therefore, in the present experiment the behavior of shorter tubings (from 1 inch to 3 feet lengths) was investigated.

It gives special meaning to the present study that this length-range - besides showing deviation from Iberall's equations - for practical purposes is the most important one because of the frequency of its application.

Chapter II

REVIEW OF LITERATURE

Solving the problem of response characteristics of the connecting system in dynamic pressure measurements is a quite complex task and has been the subject of many intricate analyses and experimental studies.

In this chapter, the more frequently used theories are briefly discussed. The available theories can be divided into two main categories: one which deals with a connecting system where the connecting passage is assumed to be rigid and the other which treats it as an elastic one.

A. Theories Concerning Rigid Wall Tubing

One simple theory (4, 5, 6, 7, 20) is based on the assumption that the flow in the connecting tube is laminar and the pressure-sensing instrument behaves in an elastic manner if the fluid medium is liquid. In this case, the pressure-sensing system consists of a passage and a volume of the pressure sensing instrument, Figure 1. The spring-loaded piston represents the flexible diaphragm of the pressure transducer. If the system is gas filled, the compressibility of the gas in the volume V becomes the major spring effect when the pressure pickup is at all stiff. Therefore, it is assumed that the volume V is enclosed by rigid walls. This setup can be treated as a lumped-parameter system if the following restrictions are met:

1. The passage length is sufficiently short so that the dead time (length of the tubing divided by the sonic velocity) can be neglected.
2. The dimensions of the pressure-sensing instrument volume must be such that the pressure in the volume may be considered uniform at any time.
3. The volume of the tubing must be small compared to the volume of the pressure-sensing instrument to assure uniform volume flow throughout the length of the tubing. This is the result of the compressibility of the gas in the pressure-sensing instrument.

The analysis consists merely of applying Newton's second law to the mass of gas in the tubing. Initially, it is assumed that $P_1 = P_2 = P_4$. The force due to the pressure P_2 is:

$$P_2 \pi d^2/4 \quad .$$

The viscous force due to the wall shearing stress is:

$$8\pi\mu\ell\dot{x}$$

where x is the displacement of the mass of the gas in the tubing. If the mass of gas moves into volume V, an amount x, the pressure P_4 will increase. The compression is assumed to occur under adiabatic conditions. The adiabatic bulk modulus E_a of a gas is given by

$$E_a = - \frac{dP}{dV/V} = \gamma P \quad .$$

The displacement x will cause a volume change

$$dV = \pi d^2 x/4 \quad .$$

This will cause a pressure change

$$P_4 = \pi E_a d^2 x/4V \quad .$$

The force due to this pressure excess is

$$\pi^2 E_a d^4 x/16V \quad .$$

Newton's law then gives

$$\frac{\pi P_2 d^4}{4} - 8\pi\mu\ell\dot{x} - \frac{\pi^2 E_a d^4 x}{16V} = \frac{\pi d^2 \ell\rho}{4}\ddot{x}$$

since

$$P_4 = \frac{\pi E_a d^2 x}{4V} \quad .$$

The final form is a second order differential equation

$$\frac{4\ell\rho V}{\pi E_a d^2}\ddot{P}_4 + \frac{128\mu\ell V}{\pi E_a d^4}\dot{P}_4 + P_4 = P_2 \quad . \tag{2.1}$$

From equation (2.1) the natural frequency ω_n and the damping ratio ζ are defined as:

$$\omega_n = \frac{d}{2}\sqrt{\frac{\pi E_a}{\ell\rho V}} \tag{2.2}$$

$$\zeta = \frac{32\mu}{d^3}\sqrt{\frac{V\ell}{\pi E_a \rho}} \quad . \tag{2.3}$$

Then equation (2.1) reduces to

$$\frac{1}{\omega_n^2}\ddot{P}_4 + 2\frac{\zeta}{\omega_n}\dot{P}_4 + P_4 = P_2 \quad . \tag{2.4}$$

The limitations of this theory are that during pressure changes both E_c and ρ vary; therefore, the natural frequency ω_n and the damping ratio ζ are not constants, that is, the system is not linear. The existence of laminar flow in the tubing during a pulse input is also questionable. For low pressure measurements the deflection of a pressure transducer diaphragm is negligible.

When the volume of the passage becomes a significant part of the total volume of a system, compressibility effects are no longer restricted to the volume of the pressure-sensing instrument alone and equations (2.2) and (2.3) become inaccurate. A more refined analysis is given in Ref. (6) where a simplified second order model is presented with the following equations for natural frequency ω_n and damping ratio ζ .

$$\omega_n = \frac{c}{\ell\sqrt{\frac{1}{2} + \frac{V}{A\ell}}} \tag{2.5}$$

$$\zeta = \frac{R\ell}{2\rho c}\sqrt{\frac{1}{2} + \frac{V}{A\ell}} \tag{2.6}$$

Thus, the undamped natural frequency ω_n and damping ratio ζ are functions of acoustic velocity c , tube length ℓ , cross-sectional area A , instrument volume V , frictional resistance R , and fluid density ρ .

Analyzing equations 2.5 and 2.6, it is apparent that with a constant instrument volume, ζ increases with line length and ω_n decreases. Similarly, with a constant length of line, increasing the instrument volume, ζ increases and ω_n decreases. Damping ratio ζ depends on fluid viscosity and density and on sound velocity, the undamped natural frequency ω_n depends only on sound velocity.

A somewhat different approach to calculating the response and lag in measuring systems subjected to steady-state sinusoidally varying pressure is discussed in Ref. (15). The pressure system is assumed to consist of an inlet restriction, tubing length, and connected instrument volume. The response of the pressure transducer is considered constant throughout the frequency range and the deflection of its flexible membrane is sufficiently small so that negligible changes occur in the internal volume. The author used the analogy of electrical wave propagation in the transmission lines. It is assumed that the air in a tubing has mass inertia, elasticity, and can dissipate energy with its motion; therefore, wave motion can be propagated along its length.

The behavior of the system is defined by the general equations for a transmission line.

$$E_2 = E_4 \cosh \sqrt{ZY}\,\ell + I_4 Z_o \sinh \sqrt{ZY}\,\ell \tag{2.7}$$

$$I_2 = I_4 \cosh \sqrt{ZY}\,\ell + \frac{E_4}{Z_o} \sinh \sqrt{ZY}\,\ell \tag{2.8}$$

where $Z = R + j\omega L$

and $Y = j\omega C$.

The quantity $\sqrt{ZY}$ may be written as

$$\sqrt{ZY} = \alpha + j\beta \tag{2.9}$$

where α is an attenuation constant determined by the decrement in pressure amplitude per length of tube and β is a propagation constant

of phase angle changes per unit length of tubing as defined by

$$\beta = \frac{2\pi f}{velocity\ of\ propagation} \quad .$$

Equation (2.7) is rewritten in the form of pressure ratio:

$$\frac{P_2}{P_4} = \cosh \sqrt{ZY}\,\ell + \frac{Z_o}{Z_4} \sinh \sqrt{ZY}\,\ell \tag{2.10}$$

or by substitution of equation (2.9) into (2.10) and simplifying, the final form of (2.10) is

$$\frac{P_2}{P_4} = \sqrt{\sinh^2 \alpha\ell + \cos^2 \beta\ell}\ \underline{/\tan^{-1}(\tan \beta\ell \tanh \alpha\ell)}$$

$$+ \frac{Z_o}{Z_4} \sqrt{\sinh^2 \alpha\ell + \sin^2 \beta\ell}\ \underline{/\tan^{-1} \frac{\tan \beta\ell}{\tanh \alpha\ell}} \quad . \tag{2.11}$$

Equation (2.11) defines the ratio of the pressure amplitude at the open end of the tubing to the amplitude existing at the instrument volume. The equation in this form requires lengthy calculation plus the attenuation constant α has to be determined experimentally. Therefore, the author uses a simplified form to calculate the pressure amplitude ratio and the resonant frequency of the system. Taback assumes negligible instrument volume and sufficiently large diameter of tubing, thus, negligible attenuation of the pressure wave occurs in the tubing; that is, α is assumed to be zero. Limitations of this theory can be summarized as follows:

1. The lack of any method for calculating α (it can be determined only experimentally using long tubing with no restriction and negligible instrument volume).
2. For accurate measurements the pressure transducer volume cannot be neglected, especially when short tubing is used.

Theory considering the damping of the occurring resonant frequencies with an inlet restriction in a connecting passage is discussed in Ref. (10). The author makes the following assumption in order to simplify the calculations.

1. The flow in the passage is one dimensional and the flow resistance can be ignored.
2. The state changes are adiabatic in the passage and the instrument volume.
3. There is no change in the volume of the pressure sensitive instrument.
4. The pressure waves in the passage propagate at constant velocity equal to the sonic velocity.

The author then uses the accoustic theory - based on the assumption of small pressure changes - to calculate the frequency response of the system. A simplified form of the system is shown in Figure 2. The following steps were used to derive the equations.

The pressure change in the reference space is assumed to be

$$P_1 = 1 + \Delta P \sin 2\pi ft \tag{2.12}$$

where P_1 is the reference atmospheric pressure and ΔP is the amplitude of periodic pressure change.

The boundary conditions at the passage inlet with throttle are defined as

$$aP_1 = aP_2 + RU_2 \quad . \tag{2.13}$$

The boundary condition at the indicator end of passage is

$$P_3 = P_4 \quad .$$

By taking $P_3 = P_4 = 1$ - on the assumption of small pressure changes - another boundary condition is given by

$$\frac{dP_4}{d(tc_o/\ell)} = \frac{1}{a}\frac{A\ell}{V} U_3 \tag{2.14}$$

where $a = 2/(\kappa - 1)$ and $U_3 = u/c_o$.

There are two kinds of pressure waves propagating in the passage. One propagates from the passage inlet to the indicator end and the other in the opposite direction. Therefore, the pressure P and velocity U are written as

$$P = 1 + A \sin[2\pi f (t - \frac{x}{c_o}) + \varepsilon A] + B \sin[2\pi f (t + \frac{x}{c_o} + \varepsilon B] \tag{2.15}$$

$$U = aA \sin[2\pi f (t - \frac{x}{c_o}) + \varepsilon A] - aB \sin[2\pi f (t + \frac{x}{c_o}) + \varepsilon B] \tag{2.16}$$

Pressure P_4 , using equation (2.12), can be written as

$$P_4 = 1 + C\Delta P \sin (2\pi f t + \varepsilon c) \quad . \tag{2.17}$$

The constants A , B , C , εA , εB , εc in equations (2.15) , (2.16) , and (2.17) are solved by introducing the pressure and velocities - at both ends of the passage (at $X = 0$, $X = 1$) which are derived from equations (2.15) , (2.16) , (2.12) , and (2.17) - into equations (2.13) and (2.14).

The final equations for the magnification of amplitude (C) and the phase lag of the pressure oscillation in the instrument volume (εc):

$$C = \left[\left(\sin\frac{2\pi f\ell}{c_o} - \frac{2\pi fV}{c_o A}\cos\frac{2\pi f\ell}{c_o}\right)^2 R^2 + \left(\cos\frac{2\pi f\ell}{c_o} - \frac{2\pi fV}{c_o A}\sin\frac{2\pi f\ell}{c_o}\right)^2\right]^{\frac{1}{2}} \tag{2.18}$$

$$\varepsilon c = \tan^{-1}\left[-\frac{\left(\sin\frac{2\pi f\ell}{c_o} - \frac{2\pi fV}{c_o A}\cos\frac{2\pi f\ell}{c_o}\right)R}{\cos\frac{2\pi f\ell}{c_o} - \frac{2\pi fV}{c_o A}\sin\frac{2\pi f\ell}{c_o}}\right] \tag{2.19}$$

and also defines the resonant frequency of connecting passage as:

$$\frac{2\pi f_r\ell}{c_o}\tan\frac{2\pi f_r\ell}{c_o} = \frac{A\ell}{V} \,. \tag{2.20}$$

Nagao (9, 10) reports the following important results of his theory and experimental work.

1. The error, resulting from the passage to the diaphragm of a pressure-sensitive instrument, increases with the decrease in the resonant frequency of the connecting passage.
2. The resonant oscillation in the connecting passage, which occurs due to the cross-sectional area of passage, can be avoided by fitting the passage with a damper such as a throttle.
3. The delay of the measured pressure change due to the damper is permissibly small.

4. The optimum throttling ratio is found to be 0.4 to 0.5 for damping the amplitude of resonant pressure oscillation and increases slightly the delay.

The previously discussed theories have their limitations as were mentioned before. By far the most detailed and complete theory is Iberall's (8). In this work Iberall first developed an elementary theory based on incompressible viscous-fluid flow. The elementary solution is then modified to take into account compressibility, finite pressure amplitudes, appreciable fluid acceleration and finite length of tubing (end effects). Account is also taken of heat transfer into the tube.

The scheme of the system is shown in Figure 3. Oscillatory pressure from the conduit 1) is applied to the entrance of the transmission tubing, and 2) the tubing has constant cross-sectional area (rigid wall) and length. The pressure-sensitive instrument is characterized by its enclosed volume V. It is assumed that 1) if the walls enclosing the instrument volume are flexible the enclosed volume can be replaced by a larger equivalent rigid volume that will store the same mass amount of fluid per unit pressure change, and 2) the pressure-sensing instrument response is independent of the frequency of expected pressure oscillation.

Deriving the elementary theory, it is assumed that:

1. Poiseuille's law of viscous resistance holds at each point in the tube.
2. The fluid is incompressible in the tube.

3. The sinusoidal pressure oscillation at the beginning of the tube is of small amplitude, compared to the mean absolute pressure.
4. If the fluid is gas it behaves isothermally in the instrument volume.

For Poiseuille's law, the following equation is written:

$$\frac{\partial P}{\partial x} = - \frac{128}{\pi} \frac{\mu_o}{d^4} Q \tag{2.21}$$

and for continuity equation,

$$\frac{\partial M}{\partial x} = - A \frac{\partial \rho}{\partial t} \quad . \tag{2.22}$$

Equation (2.21) is then differentiated with the boundary conditions ($x = o$ and $x = \ell$). A new variable is introduced: the fractional pressure excess ($\xi = \frac{P - P_o}{P_o}$). The pressure excess is then separated to vary with x and t. The ratio of the amplitude of the pressure excess at the end of the tube to that at the beginning of the tube is given by

$$\frac{\overline{\xi}_L}{\xi_o} = \frac{1}{1 + \tau\omega_a j} = \frac{1}{1 + \chi_o j} \tag{2.23}$$

where the attenuation factor $\chi_o = \tau\omega_a$; the time constant τ is defined as

$$\tau = 32 \frac{\mu_o}{P_o} \left(\frac{\ell}{d}\right)^2 \frac{V}{A\ell}$$

$\overline{\xi}_L$ is the maximum amplitude of the pressure excess at the instrument

volume and ξ_o is the amplitude of the fractional pressure excess at the origin $\xi_o = \frac{\Delta P}{P_o}$.

The real part of equation (2.23) is the attenuation in amplitude of the pressure excess and the imaginary part is the phase lag. Thus, equation (2.23) can be written as

$$\left|\frac{\bar{\xi}_L}{\xi_o}\right| = \frac{1}{(1 + \chi_o^2)^{\frac{1}{2}}} \tag{2.24}$$

$$\tan \delta_o = \chi_o$$

where δ_o is the lagging phase angle.

This simplified theory of Iberall indicates that a transmission system can be characterized by a time constant τ (function of tubing dimensions), the internal volume of pressure-sensing device, the average condition of the gas in the tubing and an attenuation factor χ_o from which the attenuation and phase lag can be computed.

In the more complex, "complete", solution Iberall removes the restrictive assumptions considered in the elementary solution. Nevertheless, a complete solution to the problem is not obtained. All first-order effects are treated to the point where the solution is correct. Only an elementary treatment is given for the second-order distortion effects. A brief discussion of the corrected theory is given below.

1. Theory corrected for compressibility - A significant difference can be noticed first in the new time constant τ_t: that it is based on the tube volume instead of the instrument volume.

$$\tau_t = \frac{A\ell}{V} \frac{\tau_o}{n}$$

where n is an exponent of "polytropic" expansion in tube. In the corrected theory the attenuation factor χ_{to} is defined as

$$\chi_{to} = \tau_t \omega_a \quad .$$

Comparing this relation to the one in the elementary theory, it can be seen that χ_{to} needs to be small in order to be valid for the elementary solution.

The ratio of the fractional pressure excess at the end of the tube $\overline{\xi}_L$ to that at the beginning of the tube ξ_o in this case is given by

$$\frac{\overline{\xi}_L}{\xi_o} = \frac{\psi_{To}}{\psi_{To} \cosh \psi_{To} + \psi_{Io} \sinh \psi_{To}}$$

where ψ_{To} is an attenuation parameter depending on the tube volume and ψ_{Io} is an attenuation parameter depending on the instrument volume. Or, in similar form as in elementary theory (equation 2.24)), the real part becomes

$$\left| \frac{\overline{\xi}_L}{\xi_o} \right| = \frac{1}{(1 + \chi^2)^{\frac{1}{2}}} \qquad (2.25)$$

2. Theory corrected for finite oscillation pressures - In this section Iberall determines the effect of finite fractional pressure excess on the attenuation in a tubing. The only assumption is that the Poiseuille velocity distribution holds. It is shown that the effect of finite pressure excess is to excite higher harmonics, resulting in a distortion of wave form and raises the mean pressure

along the tube. The higher harmonics are excited because of the nonlinearity of the equations.

The method described by Iberall in section 2 is the expansion in harmonic series. The obtained solutions are only valid for the leading term of each harmonic. By considering the solution for an infinite tube (for which only one set of boundary conditions is required), the question of convergence of the solution is discussed.

3. Theory corrected for acceleration - In the third part of the corrected section, Iberall removes the main restrictive assumption: the assumed Poiseuille velocity distribution. In order to do this, he uses the Navier-Stokes equation (equation of motion) combined with the continuity and energy equations, which represents a detailed energy balance among thermal and kinetic energies, to arrive at the Kirchoff's equation of sound. These equations are valid to first order. There is no assumption as to the form of equation of state of the fluid.

However, the result of this part of Iberall's paper is not valid for finite pressure amplitude. For this the neglected second-order term in Kirchoff's equations should be used. Therefore, it is concluded that the distortion mentioned in section 2 is valid whenever the Poiseuille regime holds.

4. Theory corrected for finite length-end effects - The end effect arises from the fact that it takes an appreciable length of tubing to set up the Poiseuille velocity distribution in the transmission lines. The character of the entrance flow is that the axial velocity is flat at the entrance, gradually developing an approximately laminar boundary layer with a core of uniform velocity until the tube is filled with laminar viscous flow.

Iberall makes the following assumption in order to solve the problem of end effect.

a. The entrance flow is incompressible.

b. The variation of pressure in radial direction in the entrance portion is negligible.

c. The quadratic terms in velocity are negligible in the boundary layer.

d. The core of the velocity distribution is potential.

Then a simplified version of equation of motion is used to find the desired result. The final result shows that the approximate effect of the entrance is to distort each input harmonic. The first-order terms are uneffected and the only equation requiring modification is the attenuated second harmonic.

Iberall presents a series of graphs for the purpose of obtaining a simple graphical solution to the line response. Four of the six graphs are based on approximate solutions, and probably much of the apparent disagreement discussed in the literature has been the cause of this approximate nature of Iberall's graphs.

In general, the restrictions applicable to Iberall's equations can be summarized as:

a. The minimum Reynolds number must be less than 2000.

b. The tube must be long enough so that the end effect can be neglected. No criterion is stated which would enable one to determine when a tube is long enough.

Iberall's equations were verified by a digital computer (16, 17) and laboratory experiments have been conducted (16). During the experiment described in (16) the restrictions mentioned under a and

b were completely fullfilled. The final conclusion of the compared results is that Iberall's equations are valid - when end effects are insignificant - to an accuracy better than 1%.

B. Theory Concerning Elastic Wall Tubing

The behavior of the pressure transmission line assuming elastic wall is discussed in Ref. (21). Womersley treats the blood vessels as a thin-walled, isotropic, elastic tube with external constraints. The analysis of the unsteady flow through a distensible vessel requires that the equations which describe both the flow and the movements of the vessel wall to be solved simultaneously. The basic flow equations for cylindrical symmetry is given by the continuity equation and the Navier-Stokes equations for an incompressible fluid. Womersley assumed: 1) under no excess internal pressure the tube has a constant radius R and wall thickness h, 2) the density of the material is ρ_w, 3) $h/R << 1$, and 4) that the radial displacements ξ and longitudinal displacements ζ at the wall and their derivatives are small to admit linear relationship. The properties of wall material are expressed by elastic modulus E_e and the Poisson's ratio ν. Since the longitudinal wall displacements are extremely small, Womersley introduced a longitudinal elastic constraint characterized by a natural frequency $\omega_n/2\pi$. The equations for the fluid and those for the wall are coupled by the condition that the fluid does not slip along the surface of the wall:

$$u = \frac{\partial \xi}{\partial t} \quad \text{and} \quad w = \frac{\partial \zeta}{\partial t}$$

for $r = R + \xi$.

Solving the prescribed equations and boundary conditions is not feasible at this time; therefore, some simplification must be carried out.

Womersley's solutions are based on the linearized equations. He considered an infinitely long tube with sinusoidal waves travelling in one direction. He neglected the nonlinear term on the basis that the velocity components are much smaller than the wave velocity in the circulatory system. He also neglected the second order term $\frac{\partial^2 u}{\partial z^2}$, $\frac{\partial^2 w}{\partial z^2}$ being very small. It is also assumed that the boundary conditions are satisfied with $r = R$, instead of $r = R + \xi$, because ξ is small compared to R . Then he obtained the solution for the pressure as

$$P = B \exp. [i\omega(t - z/c)] \tag{2.26}$$

for longitudinal wall displacement

$$\zeta = D \exp. [i\omega(t - z/c)] \tag{2.27}$$

and for radial wall displacement

$$\xi = F \exp. [i\omega(t - z/c)] \tag{2.28}$$

where B , D and F are integration constants.

The final equation for the complex wave velocity c is given as

$$c_o/c = X - iY \tag{2.29}$$

where c_o is the pulse wave velocity for perfectly elastic tubes and

is defined as

$$c_o = (hE/2R\rho)^{\frac{1}{2}} \tag{2.29}$$

and X and Y are real and imaginary values of wave velocity ratio.

The phase velocity of the waves given by c/X and Y represents the damping of the wave amplitude.

The above analysis has been restricted to waves propagating in one direction. Actually, reflected waves are also present, and the pressure measurements record superposition of advancing and receding waves. The solution for the receding wave is obtained by replacing c by $-c$; therefore, the pressure is given by

$$P = B_1 \, exp. \, [i\omega(t - z/c)] + B_2 \, exp. \, [i\omega(t + z/c)]$$

where B_1 and B_2 are the pressure amplitude of advancing and receding waves.

Chapter III

THEORETICAL ANALYSIS

The measurements of rapidly varying pressures require in most cases that the pressure sensing instrument be connected to the measuring point through a finite length of connecting tubing. The tube opening may be restricted by a connector of smaller inside diameter either because two different size tubing need to be coupled or because the response of the measuring system to the oscillating pressures must be adjusted. In most cases, exposing the pressure-measuring diaphragm to a reference pressure is necessary. This procedure requires that the diaphragm be installed so that it is exposed to a reference pressure volume which may be connected by means of tubing to a reference pressure source. The reference volume and connecting tubings is hereinafter referred to as the reference pressure system.

It will be considered that

1. The response of the pressure-sensing instrument is constant throughout the measured frequency range.
2. The deflection of diaphragm is sufficiently small so that negligible changes in internal volume occur and no energy is transferred to the reference pressure system.

In this paper the response characteristic of short transmission lines for small amplitude pressure variation is investigated. Because of the complexity of Iberall's equations, an analysis of the problem based on propagation of electrical waves on transmission lines (15, 20) is presented in this chapter.

The air column in a tube has mass inertia, elasticity, and can dissipate energy with its motion; consequently, wave motion can be propagated along its length. The behavior of the pressure system will be described in terms of the analogous electrical system by use of the electrical notations. The electrical term and the equivalent acoustical terms used herein are shown in the following table.

ELECTRICAL			EQUIVALENT ACOUSTICAL		
Term	Unit	Symbol	Term	Unit	Symbol
Voltage	Volts	V	Pressure	Psi	p
Current	Amperes	I	Volume flow	ft^3/sec	Q
Resistance	Ohms	R	Flow resistance	$lb\text{-}sec/ft^5$	R
Capacity	Farads	C	Volumetric capacity	ft^5/lb	C
Inductance	Henries	L	Inertance	$lb\text{-}sec^2/ft^5$	L

In acoustical terms the inductance per unit length of line is $L = \frac{\rho_{av}}{A}$, the capacitance per unit length is $C = \frac{A}{KP_{av}}$, and the resistance per unit length is $R = \frac{\Delta P}{Q}$.

The behavior of the system can then be defined by the general equations for a transmission line (15)

$$E_2 = E_4 \cosh \sqrt{ZY}\ell + I_4 Z_o \sinh \sqrt{ZY}\ell \tag{3.1}$$

$$I_2 = I_4 \cosh \sqrt{ZY}\ell + \frac{E_4}{Z_o} \sinh \sqrt{ZY}\ell \tag{3.2}$$

In equations (3.1) and (3.2), Z represents the sum of flow resistance and inertance or by electrical analogous the series impedance of the

system:

$$Z = R + j\omega L$$

and Y represents the volumetric capacity of the system or by electrical analogous

$$Y = j\omega C$$

The quantity $\sqrt{ZY}$ therefore is a complex number and can be written as

$$\sqrt{ZY} = \alpha + j\beta \tag{3.3}$$

where α is an attenuation constant, determined by the decrement in pressure amplitude per length of tube and β is a propagation constant or a phase-angle change per unit length of tube and can be defined as

$$\beta = \frac{2\pi f}{c}$$

The quantity Z_o indicates the characteristic impedance of the tube and can be written in the form

$$Z_o = \sqrt{\frac{Z}{Y}} = \frac{\sqrt{ZY}}{Y} = \frac{\alpha + j\beta}{Y} \tag{3.4}$$

For computation convenience, equation (3.1) can be rewritten as

$$\frac{E_2}{E_4} = \cosh \sqrt{ZY}\ell + \frac{I_4 Z_o}{E_4} \sinh \sqrt{ZY}\ell$$

and $\frac{E_4}{I_4}$ can be defined as the instrument impedance Z_4 ; thus,

equation (3.1) becomes:

$$\frac{E_2}{E_4} = \cosh \sqrt{ZY}\ell + \frac{Z_o}{Z_4} \sinh \sqrt{ZY}\ell \ . \tag{3.5}$$

Substituting equation (3.3) into equation (3.5),

$$\frac{E_2}{E_4} = \cosh (\alpha\ell + j\beta\ell) + \frac{Z_o}{Z_4} \sinh (\alpha\ell + j\beta\ell)$$

or, in another form,

$$\frac{E_2}{E_4} = \frac{P_2}{P_4} = \sqrt{\sinh^2 \alpha\ell + \cos^2 \beta\ell}\ \underline{/\tan^{-1}(\tan \beta\ell \tanh \alpha\ell)}$$

$$+ \frac{Z_o}{Z_4} \sqrt{\sinh^2 \alpha\ell + \sin^2 \beta\ell}\ \underline{/\tan^{-1}\left(\frac{\tan \beta\ell}{\tanh \alpha\ell}\right)}. \tag{3.6}$$

Equation (3.6) is the general form (15) for defining the ratio of the pressure amplitude at the open end of the tube to the amplitude existing at the pressure-sensing instrument volume. The reciprocal of this ratio is defined as the response of the system.

Even though equation (3.6) is much less complex than, for example, equations derived by Iberall (8), in practical instrumentation problems it would still require elaborate calculations. To simplify the calculations without loss of accuracy, it can be assumed in most cases that the pressure-sensing instrument volume is negligible compared to the volume of connected tubing. In most of the latest model pressure transducers, the instrument volume is very small.

With the assumption that negligible air flows at the instrument end of the tubing, the instrument impedance Z_4 approaches infinity and equation (3.5) reduces to:

$$\frac{E_2}{E_4} = \cosh \sqrt{ZY}\ell$$

or, in terms of pressure (equation 3.6)

$$\frac{P_2}{P_4} = \sqrt{\sinh^2 \alpha\ell + \cos^2 \beta\ell}\ \underline{/\tan^{-1}(\tan \beta\ell \tanh \alpha\ell)} \ . \qquad (3.7)$$

In order to determine the characteristics of resonant frequencies existing in the system, the use of a sufficiently large inside diameter tubing would result in a negligible attenuation of pressure waves; therefore, in equation (3.7) the attenuation constant α approaches zero and equation (3.7) simplifies to

$$\frac{P_2}{P_4} = \cos \beta\ell \ . \qquad (3.8)$$

In this case, the system response is a function of the applied frequency, tubing length, and the wave propagation velocity. At resonance frequencies, equation (3.8) becomes zero and the system response $\frac{P_4}{P_2}$ becomes infinite.

For determination of resonant frequencies, the following simple relationship can be derived:

$$\text{if } \frac{P_2}{P_4} = \cos \beta\ell = 0$$

$$\therefore \cos \beta\ell = 0$$

previously $\beta = \frac{2\pi f}{c}$

then for resonant frequencies:

$$\beta\ell = \frac{2\pi f_r \ell}{c} = \frac{\pi}{2}, \frac{3}{2}\pi, \frac{5}{2}\pi, \ldots.$$

where f_r is the resonant frequency of the tube with negligible instrument volume and can be defined as

$$f_r = \frac{c}{4\ell}, \frac{3c}{4\ell}, \frac{5c}{4\ell}, \ldots. \tag{3.9}$$

The wave length of a pressure wave is given by the relation:

$$\lambda = \frac{c}{f}$$

Therefore, equation (3.9) indicates that at resonance frequencies, the tube length is an odd multiple of ¼-wave length.

The problem of evaluating the effect of an added constriction at the tube inlet when the instrument volume is negligible - so that the volume flow in the instrument approaches zero - is discussed as follows. In case of restrictions which are short in length compared to one-wave length, the flow impedance consists of a resistance caused by viscous pressure losses and an inertance caused by the mass of air in the restriction. Thus, the impedance at the inlet restriction is defined (15) as

$$Z_r = \frac{\ell_r}{A_r}\left(\frac{32\mu}{d_r^2} + \frac{4}{3} j\omega\rho_{av}\right).$$

This impedance causes a pressure loss

$$P_2 - P_2' = Q_2 Z_r \tag{3.10}$$

where P_2 is the applied pressure and P_2' is the pressure applied to the tube past restriction. From equations (3.1) and (3.2) when $Q_4(I_4)$ approaches zero,

$$P_2' = P_4 \cosh \sqrt{ZY}\ell \tag{3.11}$$

and

$$I_2 = Q_2 = \frac{P_4}{Z_o} \sinh \sqrt{ZY}\ell \ . \tag{3.12}$$

Substituting equations (3.11) and (3.12) into equation (3.10),

$$P_2 - P_2' = \frac{P_4}{Z_o} \sinh \sqrt{ZY}\ell \ Z_r$$

or

$$\frac{P_2 - P_2'}{P_4} = \frac{Z_r}{Z_o} \sinh \sqrt{ZY}\ell$$

since

$$P_4 = \frac{P_2'}{\cosh \sqrt{ZY}\ell}$$

$$\frac{P_2 - P_2'}{P_2'} = \frac{Z_r}{Z_o} \tanh \sqrt{ZY}\ell$$

or in more convenient form by use of equation (3.3)

$$\frac{P_2}{P_2'} = 1 + \frac{Z_r}{Z_o} \tanh\,(\alpha\ell + j\beta\ell) \tag{3.13}$$

Equation (3.13) defines the ratio of the pressure applied to the inlet of the tube to the pressure existing in the tube past the restriction. The magnitude of the overall response of the tube and restriction can be obtained if the effectiveness of the restriction equation (3.13) is multiplied by the relation for the tube without the restriction equation (3.7).

$$\frac{P_2}{P_4} = [1 + \frac{Z_r}{Z_o} \tanh\,(\alpha\ell + j\beta\ell)](\sinh^2 \alpha\ell + \cos^2\beta\ell)^{\frac{1}{2}} \Big/ \tan^{-1}(\tan\beta\ell\, \tanh\alpha\ell) \tag{3.14}$$

From equation (3.14), it can be concluded that the effectiveness of the restriction varies with the applied frequency and the tube characteristics.

For a better visualization of the effect of the restriction in the tube to the response of the system, equation (3.13) can be written by trigonometric substitution as follows:

$$\frac{P_2}{P_2'} = 1 + \frac{Z_r}{Z_o} \left(\frac{\tanh \alpha\ell + j \tan \beta\ell}{1 + j \tanh \alpha\ell \tan \beta\ell}\right). \tag{3.15}$$

From equation (3.15), at resonance frequencies where $\beta\ell = \frac{1}{2}\pi$, $\frac{3}{2}\pi$, ... $\tan \beta\ell$ equals infinity, equation (3.15) therefore reduces to

$$\frac{P_2}{P_2'} = 1 + \frac{Z_r}{Z_o} \frac{1}{\tanh \alpha\ell}. \tag{3.16}$$

The inlet restriction needs to be applied mostly when the tubing diameter is rather large and has to be reduced to a smaller diameter tubing. In this case, as discussed previously, the attenuation constant α approaches zero and equation (3.14) reduces to

$$\frac{P_2}{P_4} = (1 + \frac{Z_r}{Z_o} \tanh j\beta\ell) \cos \beta\ell$$

or

$$\frac{P_2}{P_4} = \cos \beta\ell + j \frac{Z_r}{Z_o} \sin \beta\ell \tag{3.17}$$

If the inside diameter of the applied constriction is small, the impedance is almost pure resistance since the viscous forces which cause pressure losses are much larger than the inertia forces caused by the mass of air in the constriction. The ratio of the impedance $\frac{Z_r}{Z_o}$, therefore, closely approaches a real number and equation (3.17) can be rewritten in polar coordinates

$$\frac{P_2}{P_4} = [\cos^2\beta\ell + (\frac{Z_r}{Z_o} \sin \beta\ell)^2]^{\frac{1}{2}} \underline{/\tan^{-1}(\frac{Z_r}{Z_o} \tan \beta\ell)} \tag{3.18}$$

in the special case, when the impedance ratio $\frac{Z_r}{Z_o} = 1$, equation (3.18) reduces to

$$\frac{P_2}{P_4} = 1\underline{/\beta\ell} \tag{3.19}$$

Analyzing equations (3.16) and (3.18), the important conclusion can be seen: the restriction at the tubing inlet is extremely effective in

reducing large amplitude resonances as verified also by Refs. (1, 9, 10, 15). The delay is hardly increasing when the proper restriction ratio (optimum between 0.4 to 0.5, Ref. (10) is used. A large diameter tubing with the proper inlet restriction is more effective in reducing the resonant frequencies and secures a unit response over a large frequency range, than a small diameter tubing would, which causes considerable attenuation at higher frequencies. Analysis of pressure system with instrument volume is presented in the appendix.

The remaining part of this chapter discusses the problem of the elastic property of the tubing. When the system is liquid-filled, it is quite often possible that the flexibility of the tubing gives rise to a compressibility comparable to that of the liquid. The simplest way to take into account the flexibility of the tubing is to define and replace the compressibility of the liquid by an effective value $\overline{b}$ and $\overline{K}$ (Ref. 8). The effective compressibility factor $\overline{b}$ for a liquid, taking into account the elastic property of the tube, becomes then

$$\overline{b} = b + \frac{P_o - P_a}{E} \frac{d}{h} \tag{3.20}$$

and the effective compressibility of a liquid $\overline{K}$ is

$$\overline{K} = K + \frac{P_o - P_a}{P_o} \frac{d}{E} \frac{}{h} \tag{3.21}$$

where P_o = mean liquid pressure,

P_a = ambient external pressure (usually atmospheric),

E = elastic modulus of the tubing material, and

h = wall thickness of the tubing.

Equations (3.20) and (3.21) have assumed that the thickness of the tubing wall is small compared to the tubing diameter. However, the effect of the tubes' elastic property on the compressibility as expressed in equations (3.20) and (3.21) are extremely small.

Chapter IV

EXPERIMENTAL EQUIPMENT AND TECHNIQUE

The pressure transmission lines from the point where the pressure is being measured to the pressure sensing instrument play an important role in dynamic pressure measurements. In order to obtain the maximum dynamic performance, a flush diaphragm pressure transducer mounted directly at the point of the pressure measurement is desired, if at all possible, since any connecting tubing or volume chamber will degrade performance to some extent. When this is not possible, the use of transmission lines cannot be avoided.

Theories discussed in Chapter II describe the behavior of pressure transmission lines. Those theories have been experimentally verified. However, tubings of short lengths (less than four feet) show considerable deviation from predicted values. The purpose of this experiment is to provide sufficient and reliable data to clarify the behavior of short connecting tubings exposed to pulse input.

The use of commercially available and most frequently used pressure transducers and connecting tubings were emphasized throughout this research. The experiment also intends to relieve the problem of calculating dynamic pressure without involving the complex equations concerning this phenomenon.

The experiment discussed in this chapter was made in the Fluid Dynamics and Diffusion Laboratory at Colorado State University.

A. Production of Pulsating Pressure

For higher accuracy of the measurements, the usage of precisely controlled pressure pulse was desirable. A mechanical device which generates such a pulse was constructed from delrin and is shown in Figure 6. Its frequency range is limited, of course, but was sufficient for this experiment. This pulse generator consists of a valve housing with a pressure inlet- and outlet-port and a rotating valve with the shaft supported by two ball bearings. The disc, which served as the rotating valve to control the air flow, has four intercrossing passages drilled precisely at 45^0 from each other. The line of the (inlet + outlet) ports lies in the plane of these passages, thus, assuring perfect alignment of the ducts in the proper phases of the rotation, yielding eight pressure pulses per revolution.

Care was taken to keep the air gap between rotor and valve housing down to a minimum for smallest possible air leakage. Escaping pressure could cause a disturbance and amplitude variation in the delivered pressure pulses. The rotating valve turns freely in the housing, thus, avoiding heat build-up in the system which would affect the output signal of the pressure transducer.

The shaft of the rotating valve was connected to a Barber Colman permanent magnet D.C. motor. This motor is equipped with a gear box, reducing the motor speed to 2250 RPM at full voltage. The motor was powered from a 30V D.C. variable voltage power supply. The construction of the motor enables it to vary its speed by altering the input voltage, thus obtaining the desired frequencies.

The wave form from the pulse-function generator is shown in Figures 6b and 6c as it appeared on the dual beam oscilloscope (Tektronix Type 502A) which was used throughout this experiment. At low frequency, the oscilloscope trace shows the true output of the pulsator; however, from approximately 120 cps the output wave form is sinusoidal.

B. The Pressure Detecting System

The arrangement of the pressure detecting system and the scheme of experiment setup is illustrated in Figures 7 and 5, respectively.

Two identical Statham unbonded strain gage type pressure transducers Model P22 with a range of 0-1 psi was used for this experiment. The inner construction of this type of pressure transducer consists of a flexible diaphragm mechanically connected to a movable frame with four filaments of strain sensitive resistance wire and an instrument volume (0.073 cu. inch). The filaments are of equal lengths and are arranged in the form of a Wheatstone bridge. High resonant frequency did not appear in the response of the pressure transducers to pulse input within the frequency range 0-300 cps. Therefore, it was concluded that the natural frequency of pressure transducers were above the tested frequency range.

The inlet ports of the pressure transducer were connected to a manifold made of the same size brass tubing as the inlet ports, keeping the distance from the center of manifold to the pressure transducer at a practicable minimum (about 1 inch, Figure 37). The manifold is connected through a 5/16-inch I.D., 6-inch long heavy wall Tygon tube to a 1/16-inch DIA. inlet port embedded in a vertical wall. The

5/16" x 6" tube served as a pressure equalizing chamber to make certain that equal pressure passes through the manifold to the pressure transducers.

In order to assure that the two pressure transducers' output are identical throughout the frequency range, a control unit was built for each transducer, Figure 4, Nos. 9, 10. The schematic diagram is shown in Figure 8. A 3V D.C. power supply, Figure 4, No. 7, excites the transducers' strain-gage bridge. With no pressure the bridge output can be zero balanced by adjusting the variable resistor of zero adjust. The pressure transducer output can be controlled by adjusting the variable resistor of sensitivity adjust. This enables one to balance the two transducers to deliver identical output signals when connected to the same pressure source.

Proof of identical functioning of the two adjusted pressure transducers connected directly to the manifold is illustrated in Figures 9 and 10 by the super imposed signal waves on the dual beam oscilloscope for several frequencies.

During the experiment the transducer kept as reference was attached directly to the manifold and the other was connected with the tubings to be tested (Figure 12).

The pressure transducers were calibrated with a Meriam water manometer (type W, model 30 EB 25) and a pitot static tube served as a pickup. The calibration curve is shown in Figure 11.

The 1/16-inch diameter inlet hole in the wall was chosen arbitrarily. Several different sizes from 1/32-inch to 1/8-inch DIA. were tested and no effect on the quality of wave output was found.

C. Readout Instruments

The output voltage of the pressure transducers was fed directly into a dual beam oscilloscope (Figure 5, No. 5) Tektronix model 502 A; thus, the two output wave forms were observed simultaneously. The traces were photographed by a polaroid camera and the pictures were used to calculate the phase shift.

The output signals from the pressure transducers, led through a distributor switch, were fed into a preamplifier (Figure 5, No. 3) Tektronix, type 122 having a gain of 1000. The signal from the preamplifier then was fed into a RMS voltmeter (Figure 5, No. 2) and into an electronic counter (Figure 5, No. 6), HP 523 B for the exact determination of the frequency. The RMS voltmeter measured the RMS values of the pressure transducers ouput signals. The introduction of the high gain amplifier was needed to trigger the electronic counter. The output voltage of the pressure transducers was in the order of millivolts; therefore, the waves observed on the oscilloscope and recorded in the pictures were unamplified.

D. Measurement Procedure

The scheme of the complete test setup is shown in Figure 5 and the instruments used in Figure 4. The test procedure was as follows. The air pressure was regulated to generate waves with amplitude identical to one shown in Figures 9 and 10 each time a run was started; therefore, in all measurements the pressure input was constant. The pulse generator outlet port was held against the 1/16-inch DIA. inlet port of the pressure chamber (Figure 4, No. 13 and Figure 7). The gap was 0.020 inches.

During the adjustment of two pressure transducers for the same output at various frequency ranges, it was found that the construction of the manifold was extremely important in order to obtain two identical outputs. The slightest asymmetry caused considerable difference in the pressure transducers output. Therefore, before each run the pressure transducer #2 (Figure 4, No. 11) was calibrated against the reference pressure transducer #1 (Figure 4, No. 12). After calibration, the tube to be tested was placed between the manifold outlet port and pressure transducer inlet port (Figure 12).

Various lengths and I.D. of flexible "Tygon" tubings formulation R3603, manufactured by U. S. Stoneware Co., were tested. Tubings 1/8-inch I.D. and up were connected by using couplings with constant I.D. (0.035 inch), length (.565), and variable O.D.'s to fit the test tubings. The other end of the coupling was made the same O.D. as the pressure transducer inlet port; thus, the connection with a piece of flexible tubing was easily obtained.

Tubings less than 1/8-inch I.D. were connected directly over the manifold and pressure transducer ports.

By varying the D.C. motor revolution (Figure 4, No. 14), the desired frequency from the pulse generator was obtained. The pressure transducer signals were observed on the dual beam oscilloscope (Figure 4, No. 5) and were recorded by a polaroid camera. The signals through a double pole switch (Figure 4, No. 8) through the preamplifier (Figure 4, No. 3) were read on the RMS voltmeter (Figure 4, No.2) and the frequency of pulses counted on the electronic counter (Figure 4, No. 6).

The purpose of the switch was to record both pressure transducer signals on the same RMS voltmeter by switching from one signal to the

other, thus, avoiding the chance of error caused by possible differences between instruments.

No special temperature measurements were taken because the entire test was made at room temperature thermostatically controlled within $\pm 1^{0}C$.

In the electrical system, only the oscilloscope was grounded. All cables carrying the signals of pressure transducers were shielded to avoid the noise pickup.

Chapter V

ANALYSIS OF DATA

Data obtained by the technique described in Chapter IV is analyzed in this chapter. This analysis emphasizes comparison between the simplified theory discussed in Chapter III and the result of this experiment.

The result of this analysis may be used as a reference in most practical cases when high accuracy of the solution is not absolutely necessary. The experimental data can be analyzed from the following points of view:

1. Simple tube system with negligible instrument volume, no inlet restriction.
2. Tube system with inlet restrictions.
3. Test results of the elastic tubings.
4. Phase shift analysis.

A. Simple Tube System with Negligible Instrument Volume, No Inlet Restriction

For this test, relatively small inside diameter tubings were selected to fit over the thin inlet port of the pressure transducer and the manifold to avoid the use of a coupling which might act as an inlet restriction.

Three pieces of tubings were tested - all the same length (3 ft) but different I.D. (3/32", 1/16", and 0.052"). Their amplitude ratio versus frequency is plotted in Figure 13. The plot of the 3/32" I.D.

tubing shows clearly the first resonant peak at 15 cps but its amplitude is only 1.05 magnitude (Figure 24). Due to the larger DIA, its attenuation is less steep compared to the two smaller DIA tubings. The 1/16" I.D. showed a high amplitude amplification (1.13) at the first resonance frequency region, around 30 cps (Figure 25). It has steeper attenuation until approximately 120 cps compared with the larger DIA tubing.

I.B.M. computer program was written to calculate a 1/16" inside diameter, 3-ft long tubing response for different value of α using equation (A.2), taking into account the volume of the pressure transducer. The resonant peaks appearing at low frequency are well predicted by equation (3.6) (Figure 39) for small diameter tubing with no inlet restriction.

The low amplitude of the resonance frequency of the tubing with 3/32" I.D. is probably caused by inlet restriction effect due to the size difference between the manifold outlet (and the pressure transducer inlet, respectively) and the tubing I.D. even though no extra coupling was used.

Theories (10, 15) predict that no resonance frequency occurs when the tubing I.D. is sufficiently small. This experiment indicates that the 1/16" I.D. tubing has a large resonant peak; therefore, it cannot be considered "small" enough. The 0.052" I.D. tubing shows very small (1.01) resonant peak; therefore, it can be considered sufficiently "small" to damp the first resonant peak.

The occurrence of the first resonant peak in the 1/16" I.D. tubing can be analyzed more in detail in Figure 14, where the amplitude ratio of different length tubings are plotted against frequency. Different

tube lengths produce different amplitude resonant peaks. The magnitude of the resonance peak is a maximum for a tube length of 12 inches, where the magnification factor is 1.25 (Figure 26). Decreasing the tube length below 12 inches causes the amplitude of the resonance frequency to become more and more flat until the pressure P_4 equals P_2. This amplitude decrease is very gradual and even for a one-inch tube length an amplitude still exists (Figure 27).

Attenuation of the 1/16" I.D. tubing is in good agreement with the predicted values (Figure 39) after the first resonance peak is increasing rapidly. The frequency where the unity line is crossed increases as the tube length becomes shorter. Three-ft long tubings with I.D. less than 1/16" show very rapid attenuation (Figure 13).

It should be noted that the appearance of the resonance peaks at high frequency is relatively uneffected by the length and I.D. of the tubing or by any coupling effect (Figures 13 and 14). The magnitude of the peak shows slight sensitivity towards I.D. of the tubing and diminishes with the decrease of tube length and with the increase of I.D. of the tubing. All this resonance peaks start around 240 cps (Figure 28), reach maximum at approximately 270 cps (Figure 29), and decrease gradually at higher frequencies. A comparison of Figures 28 and 29 clearly shows the increased pressure in the tubing between frequencies 240 and 270 cps.

B. Tube System with an Inlet Restriction

In the test procedure, tubings larger than 3/32" I.D. were connected to the pressure transducer and the manifold by means of couplings. Thus, the system could be treated as one with an inlet

restriction. The length and I.D. of the couplings were kept constant (ratio of .062) throughout the experiment.

The response of various I.D. tubes with connector, all the same length (3 ft) are shown in Figure 15. Neither of the plots showed any first resonance frequency which was predicted in theory equations (3.16) and (3.18); that is, the inlet restriction reduces the first resonance frequency (Figure 30). However, the coupling effect does not prevent the occurrence of resonance peaks at higher frequencies (270 cps). The magnitude of these peaks is a function of the tube I.D., it is inversely proportional to the inside diameter of the tubing (Figures 31, 32, and 33). The attenuation has an increasing gradient with increased tubing inside diameter until about 60 cps. From there on it becomes nearly linear to about 220 cps.

Amplitude ratio is plotted against frequency for several tube lengths below 3 ft in Figure 16, 1/8" inside diameter and Figure 17, for 1/4" inside diameter. These curves do not show a first resonance frequency, but a peak at high frequency is present in all. Comparison between Figures 16 and 17 show an important result. The 1/8" inside diameter tubing is much more suitable for practical application. The attenuation is hardly effected by the length of the tube and the curves are very close to each other. The value of the amplitude ratio approaches one as the length of the tubing becomes shorter (one inch). The attenuation is very gradual and almost linear up to 220 cps. The curves on Figure 17 are more dispersed. Due to the larger diameter, the attenuation is much more sensitive to the changes of tube length. The value of the amplitude ratio is one only for very short tubings (one inch) until approximately 38 cps.

The result of the test proves that couplings serving as inlet restrictions are very effective in reducing the first resonance frequency, while they do not cause any noticeable change to resonance peaks at high frequency.

C. Test Result of Elastic Tubing

Experiments were run to determine possible effects of the elastic properties of commercially available tubings on the pressure pulse response. The setup of the previous experiments was used; the system was air filled with the pressure kept approximately 1/2 psi. Instrument volume was negligible.

Comparative studies were done on tubings of different materials but constant inside diameter (1/8") in two different lengths, 3 ft and 10 in.:

1. rigid wall tube
2. flexible 1/16" wall, Tygon tubing*
3. flexible 1/32" wall, rubber tubing.

Amplitude ratio versus frequency of the above mentioned tubing is shown in Figures 18 and 19.

The result indicates that - under tested pressure (1/2 psi) and frequency range (0-300) - no significant difference between the most flexible rubber tubing and the more stiff Tygon tubing. Their curves are almost identical. However, some deviation from the rigid wall tubing exists. This is probably due to the different coupling solution which had to be applied to connect the rigid wall tubing to the pressure transducer and to the manifold.

*Tygon tubings with the thinest available wall (1/32") were compared with heavier (1/16") over a large range of tube length and I.D. No noteworthy difference was found.

D. Phase Shift Analysis

The phase relations were calculated from the traces appearing on the dual beam oscilloscope. A plot of this phase shift versus frequency for various tubing I.D.'s having the same length (3 ft) is illustrated in Figure 21. These curves show that the following general characteristics are common to the response curves (Figure 20). The phase angle shifts very slowly until the first resonance frequency is reached. Almost no lag can be detected in the frequency range up to 10 cps (Figure 34). From thereon a rapid change occurs until it reaches about 70^{o} at approximately 40 cps (Figure 35). Then for a short frequency range (40-60 cps) the phase shift remains almost constant. The lag from thereon increases. The rate of change of lag-angle with increasing frequency becomes more and more linear as the amplitude ratio becomes nearly linear. The second detected resonance frequency does not affect the linearity of phase lag. In case of a shorter tubing (approximately 1 ft) (Figure 22), the phase lag shows more linearity during first resonance frequency; however, it becomes nonlinear as the frequency increases. During the second resonance frequency the phase lag decreases (Figure 36).

E. Summary of Analysis

A general plot of the response of all 3-ft long flexible and rigid wall tubes is shown in Figure 20. Tubes with small diameter which were free from inlet restrictions show first resonance peaks predicted by the theory. The tube with large I.D. where a coupling had to be used and thus was treated as a tube system with inlet restriction shows no first resonance frequency. The coupling, therefore, is very effective in damping the resonance frequency as mentioned in (1, 8, 10, 15).

Tubing with inside diameter less than 1/16" are free from first resonance peaks, but their attenuation is progressing rapidly with the increase of frequency up to 100 cps. The above experimental results were well predicted by the simplified theory discussed in Chapter III.

The appearance of resonance peaks at higher (270 cps) frequencies are not affected by either an inlet restriction or very small diameter and/or length of the tubing. The response curves which were calculated from equation (3.6) (Figure 39) indicates no resonance frequency in this range. These peaks appeared always in the same frequency range regardless of the tubing geometry. Therefore, it was concluded that this is the resonant frequency of the system and it is independent of the tested tubing. Because of the high frequency at which it sets in, no special investigation was made to define them.

No commercially available tubings, including the most flexible 1/32" walled, showed any elastic property at tested pressure (1/2 psi) and frequency range (0-300).

Chapter VI

CONCLUSIONS

The response characteristics of short pressure lines to pulse input were experimentally investigated. The results of the experiment are summarized as follows:

1. For low air pressure applications commercially available, flexible tubings can be treated as rigid wall tubes.
2. To obtain flat response, the shortest possible tube should be used.
3. In order to avoid the phenomenon of low frequency resonant peak, either small inside diameter tubing less than 1/16 inch or larger I.D. with inlet restriction, should be employed.
4. Small I.D. tubings, 1/16 inch and less, have considerable attenuation up to 120 cps. Tubes of large inside diameter of 1/4 inch with inlet restrictions showed progressed attenuation to approximately 60 cps.
5. For practical applications where various tube lengths are required, the optimum is found to be 1/8-inch I.D. with inlet restriction to reduce resonance frequency. The effect of the length on the response is minimum at this diameter. Slight attenuation takes place.
6. Pressure is slightly affected by the tube characteristics between 120 and 220 cps (Figure 24).

7. The lack of a method for calculating the attenuation constant α, limits the general application of the equations discussed in Chapter III. The value of α is critical in computation of the response curves (Figure 39).
8. In case of short length tubing of 1/2 - 3 ft after the first resonance peak, the phase lag is nearly linear. In case of very short tubing, 2 inches and less, the lag becomes non-linear and tends to shift toward zero with the increase of frequency.

The experiment is of use for dynamic pressure measurements at the described range where the existing theories are inaccurate.

BIBLIOGRAPHY

1. Baretto, G. and Steward, W. G., Dynamic response of pressure lines. Note prepared for a course on Instrumentation for Fluid Mechanics Research, Dr. E. J. Plate, Instructor.

2. Barton, J. R., A note on the evaluation of designs of transducers for the measurement of dynamic pressures in liquid systems. Statham Laboratories Instrument Notes, No. 27, 1954.

3. Corcos, G. M., Pressure measurements in unsteady flow. Symposium on measurement in unsteady flow, ASME Hydraulic Division Conference, 1962.

4. Delio, G. J., Schwent, G. V., and Cesaro, R. S., Transient Behavior of Lumped-Constant Systems for Sensing Gas Pressures. NACA Technical Note No. 1988, 1949.

5. Doebelin, E. O., Measurement Systems: Application and Design. McGraw-Hill Book Company, 1966, p. 391-406.

6. Hougen, J. O., Martin, O. R., and Walsh, R. A., Dynamics of Pneumatic Transmission Lines. Control Engineering, p. 114, 1963.

7. Hubbard, P. G., Interpretation of Data and Response of Probes in Unsteady Flow. Symposium on Measurements in Unsteady Flow, ASME Hydraulic Division Conference, 1962.

8. Iberall, A. S., Attenuation of Oscillatory Pressures in Instrument Lines. Natl. Bur. Std./U.S./, Res. Paper RP 2115, July ASME Trans., 1950.

9. Nagao, F. and Ikegami, M., Errors of an Indicator Due to a Connecting Passage. Bull. JSME, vol. 8, no. 29, 1965.

10. Nagao, F., et al., Influence of the Connecting Passage of a Low Pressure Indicator on Recording. Bull. JSME, vol. 6, no. 21, 1963.

11. Rudinger, G., Review of Current Mathematical Methods for the Analysis of Blood Flow. Biomedical Fluid Mechanics Symposium, ASME, Fluids Engineering Conference, Denver, Colorado, 1966.

12. Schweppe, et al., Methods for the Dynamic Calibration of Pressure Transducers. Natl. Bur. Std./U.S./, Monograph 67, 1963.

13. Stedman, C. K., Alternating Flow of Fluid in Tubes. Statham Laboratories Instrument Notes, No. 30, 1956.

14. Stein, P. K., Measuring Fluctuating Pressure. Instruments and Control Systems, p. 156, September, 1964.

15. Taback, I. The Response of Pressure Measuring Systems to Oscillating Pressures, NACA, Technical Note 1819, 1949.

16. Watts, G. P., An Experimental Verification of a Computer Program for the Calculation of Oscillatory Pressure Attenuation in Pneumatic Transmission Lines. U. S. Atomic Energy Commission, Los Alamos Scientific Laboratory of the University of California, Los Alamos, New Mexico, Contract W-7405 - Eng-36, 1965.

17. Watts, G. P., The Response of Pressure Transmission Lines. U. S. Atomic Energy Commission, Los Alamos Scientific Laboratory of the University of California, Los Alamos, New Mexico, Contract W-7405-Eng-36, 1965

18. White, G. E., Response Characteristics of a Simple Instrument. Statham Laboratories Instrument Notes, No. 2, 1948.

19. White, G. E., The Meaning of "Natural Frequency". Statham Laboratories Instrument Notes, No. 12, 1949.

20. Wildhack, W. A., Pressure Drop in Tubing in Aircraft Instrument Installations, NACA, Technical Note 593, 1937.

21. Womersley, J. R., An Elastic Tube Theory of Pulse Transmission and Oscillatory Flow in Mammalian Arteries. Wright Air Development Center, W.A.D.C. Report TR 56-614, 1957.

APPENDIX

APPENDIX

In Chapter III detailed theoretical anlysis is given to determine the general response of pressure transmission lines to pulse input. The theory is then simplified, assuming negligible instrument volume. The response of flexible tubing was determined experimentally using identical pressure transducers. Even though the reference pressure transducer was kept at a practicable minimum distance (1 inch) from the center of the manifold, it did not measure the true pressure existing in the manifold. It is of interest to know the degree of pressure change in case of such short connecting passage.

Because of the small volume of the connecting tubing, the internal volume of the pressure transducer cannot be neglected. The instrument impedance in such cases is a function only of its volumetric capacity and can be written

$$Z_4 = \frac{1}{j\omega C_4} = \frac{\kappa P_{av}}{j\omega V_4} \quad .$$

The characteristic impedance of the tubing as given by equation (3.4) is

$$Z_o = \frac{\alpha + j\beta}{Y} = \frac{4(\alpha + j\beta)\, \ell \kappa P_{av}}{j\omega \pi D^2 \ell} \quad .$$

The ratio of these impedancies is

$$\frac{Z_o}{Z_4} = \frac{4V_4}{\pi D^2 \ell} \left[(\alpha\ell)^2 + (\beta\ell)^2\right]^{\frac{1}{2}} \underline{/\tan^{-1} \frac{\beta}{\alpha}} \qquad \text{(A.1)}$$

This impedance ratio appears in equation (3.6) and its value depends on the ratio of the pressure transducer volume to the total volume of the passage. Equation (3.6) is altered to include equation (A.1), only the values of real quantities and phase angles,

$$\frac{P_2}{P_4} = (\sinh^2 \alpha\ell + \cos^2 \beta\ell)^{\frac{1}{2}} \underline{/\tan^{-1}(\tan \beta\ell \tanh \alpha\ell)}$$

$$+ \frac{4V_4}{\pi D^2 \ell} [(\alpha\ell)^2 + (\beta\ell)^2]^{\frac{1}{2}} (\sinh^2 \alpha\ell$$

$$+ \sin^2 \beta\ell)^{\frac{1}{2}} \underline{/\tan^{-1}\left(\frac{\tan \beta\ell}{\tanh \alpha\ell}\right) + /\tan^{-1}\left(\frac{\beta}{\alpha}\right)} . \qquad \text{(A.2)}$$

Equation (A.2) defines the ratio of the pressure amplitude at the manifold end of the passage to the amplitude existing at the pressure transducer volume.

In order to apply equation (A.2) to the reference pressure system, the value of α had to be determined experimentally. In Chapter III α was defined as an attenuation constant determined by the decrement in pressure amplitude per length of tubing. In this present work α was determined for a 0.035-inch inside diameter tubing (same I.D. as the pressure transducer and manifold ports), 1 1/8-inch long. It was found to vary with the square root of the applied frequency. Its value is $0.022 \sqrt{f}$. Value of β was calculated from the velocities of propagation in different I.D. tubings given in Figure 5, Ref. (15). The value of free-air velocity was rounded off to 1000 ft/sec. The pressure transducer internal volume was 0.073 cubic inch, length of the passage 1 inch and the inside diameter of the passage was 0.035 in ch.

An I.B.M. computer program was written to calculate the reference pressure system response, using equation (A.2) for a frequency range 0-300 cps. The result of the calculation is presented in Figure 38.

The computation was accomplished by a C.D.C 6400 computer at Colorado State University Computer Center.

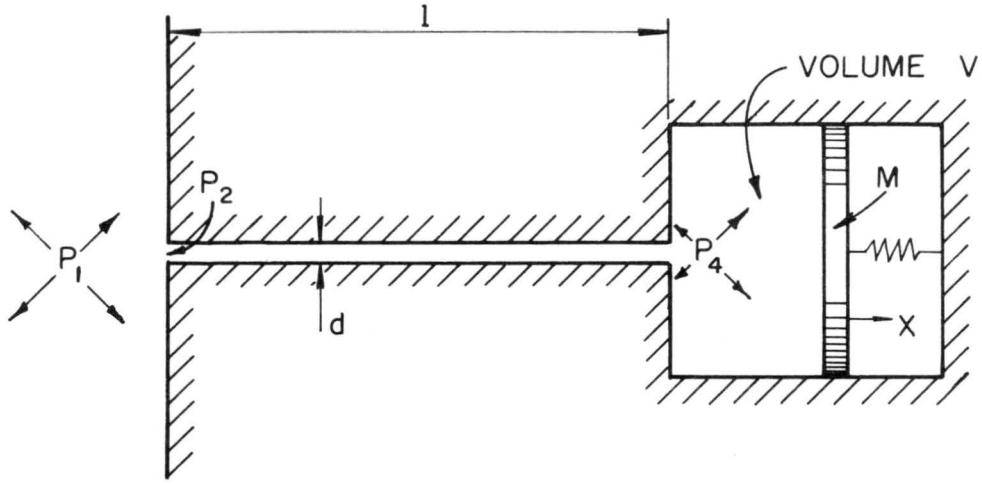

Figure 1. Pressure sensing system with flexible diaphragm

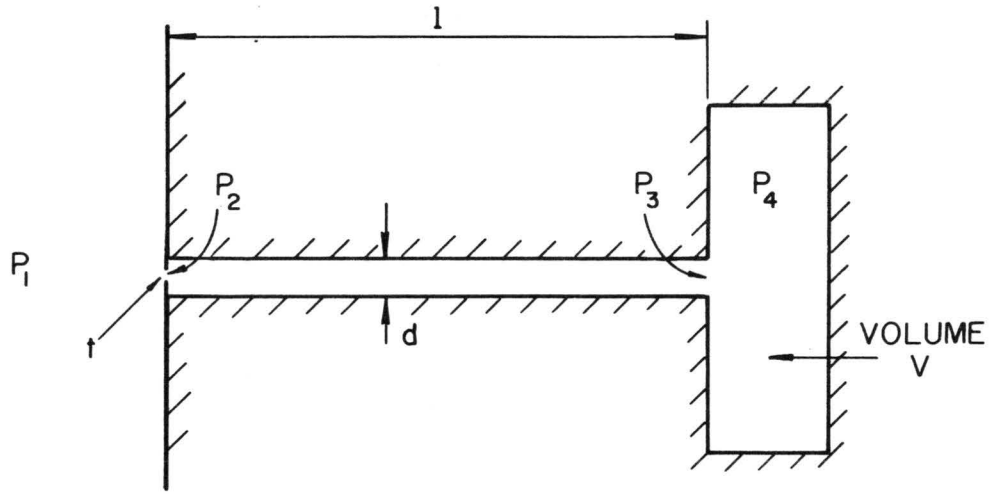

Figure 2. Pressure system with throttle fixed at the passage inlet

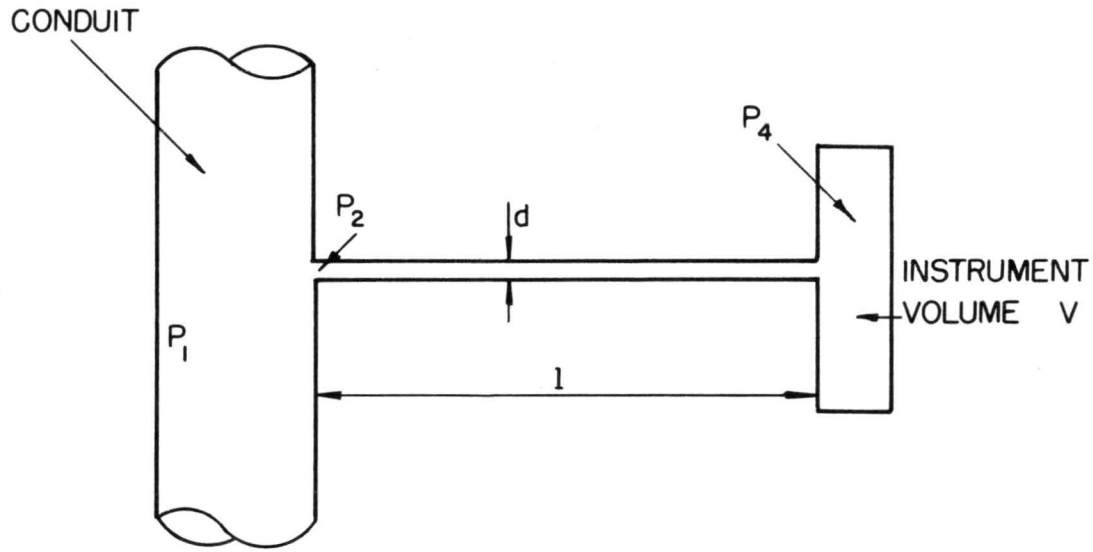

Figure 3. Schematic diagram of a fluid transmission system

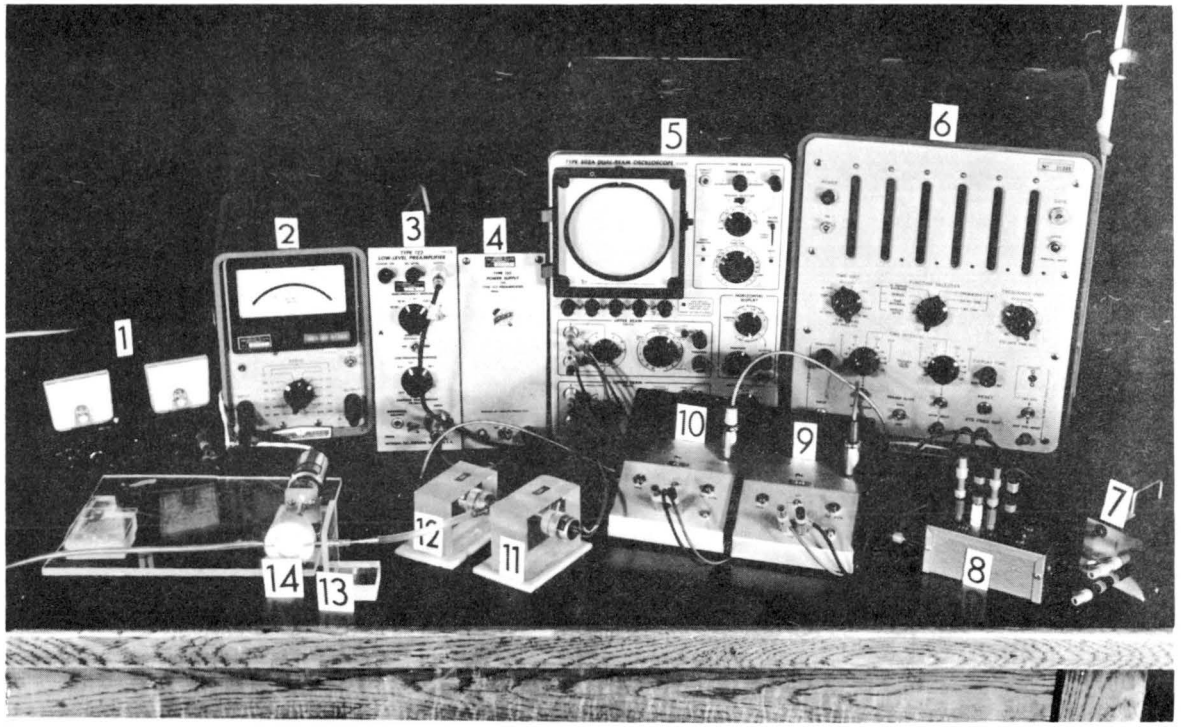

Figure 4. Pressure sensing and readout system

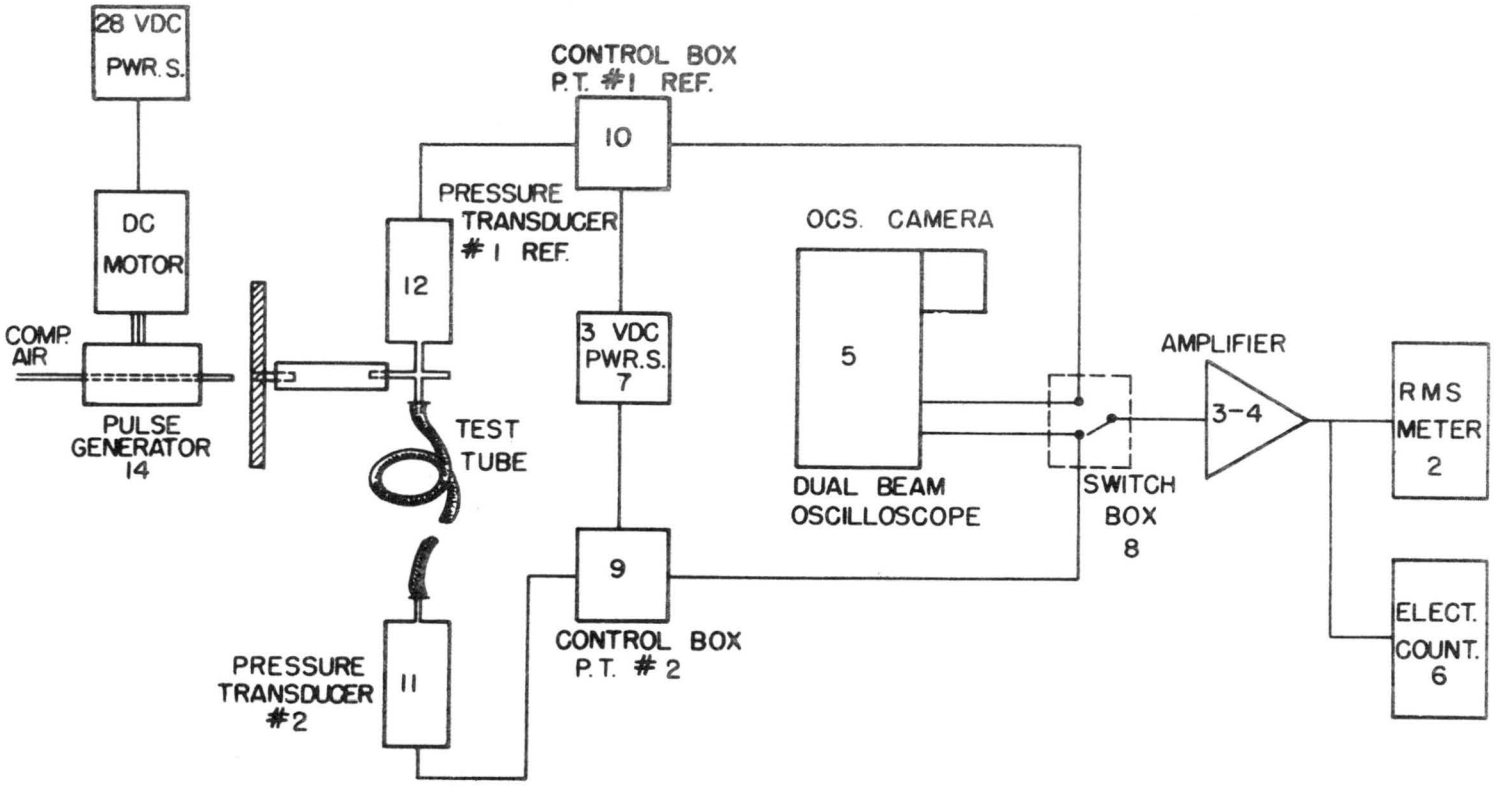

Figure 5. Schematic of experiment setup

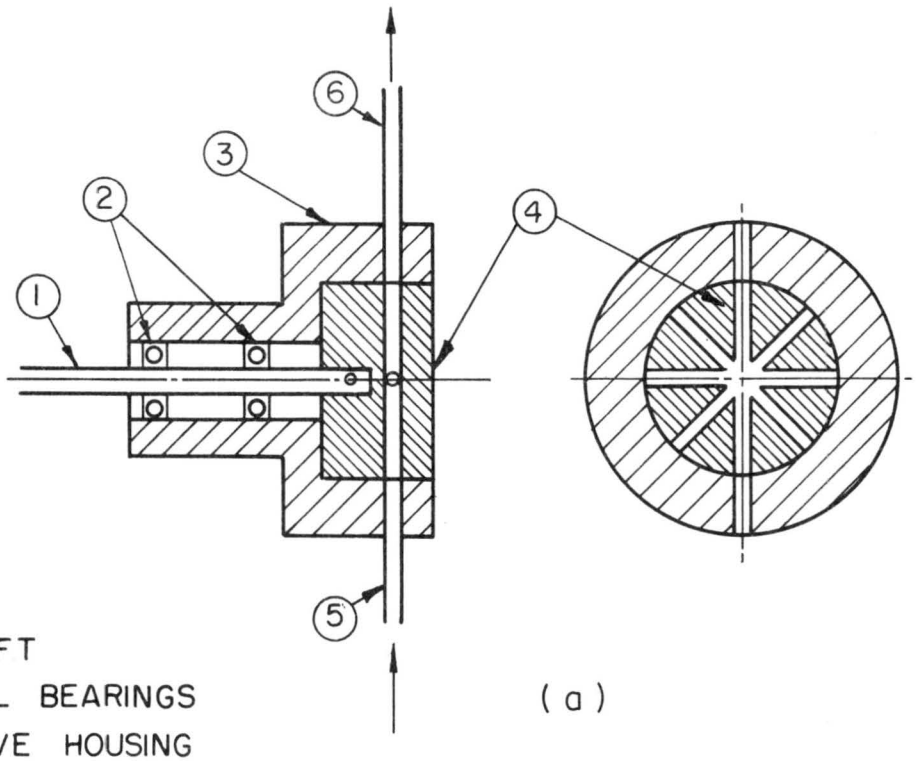

1. SHAFT
2. BALL BEARINGS
3. VALVE HOUSING
4. ROTATING VALVE
5. PRESSURE INLET PORT
6. PRESSURE OUTLET PORT

(a)

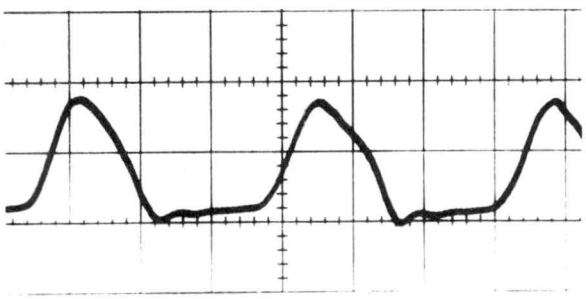

(b)

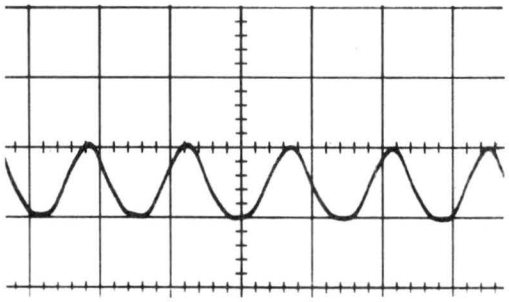

(c)

Figure 6. Rotating valve pulse-function generator
a) Constructional features of pulsator
b) Output wave form at low frequency
c) Output wave form at high frequency

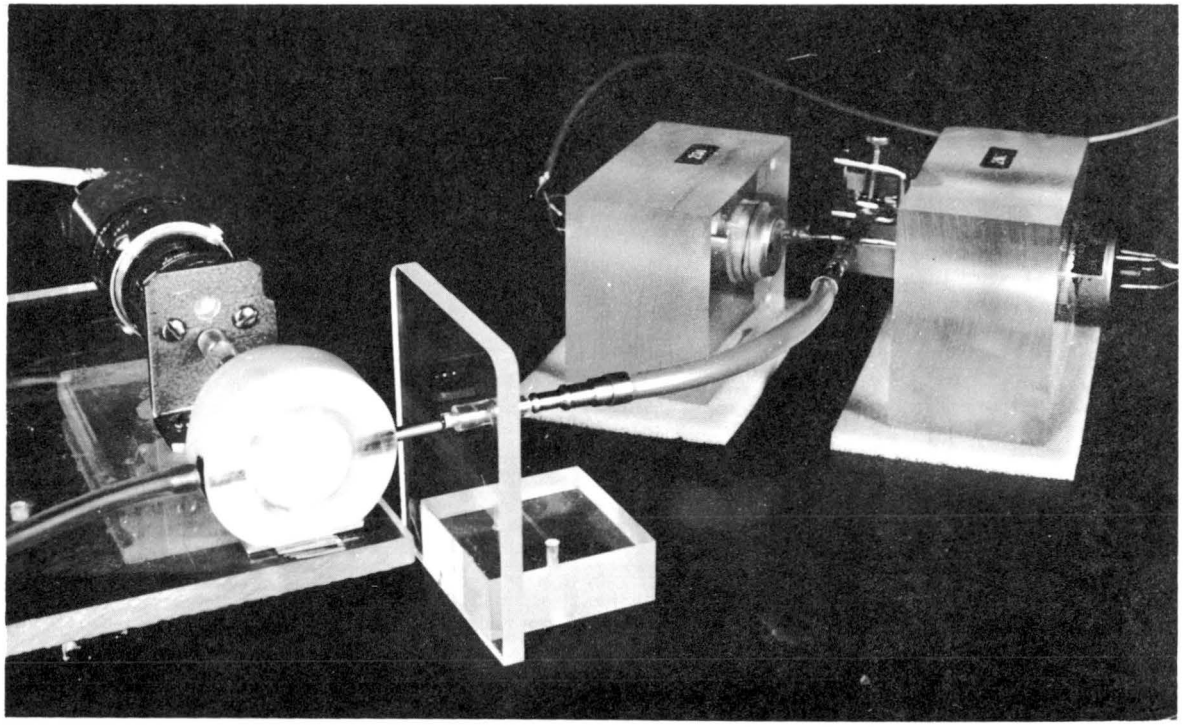

Figure 7. Pressure pulse generator and pressure detecting system in calibration position

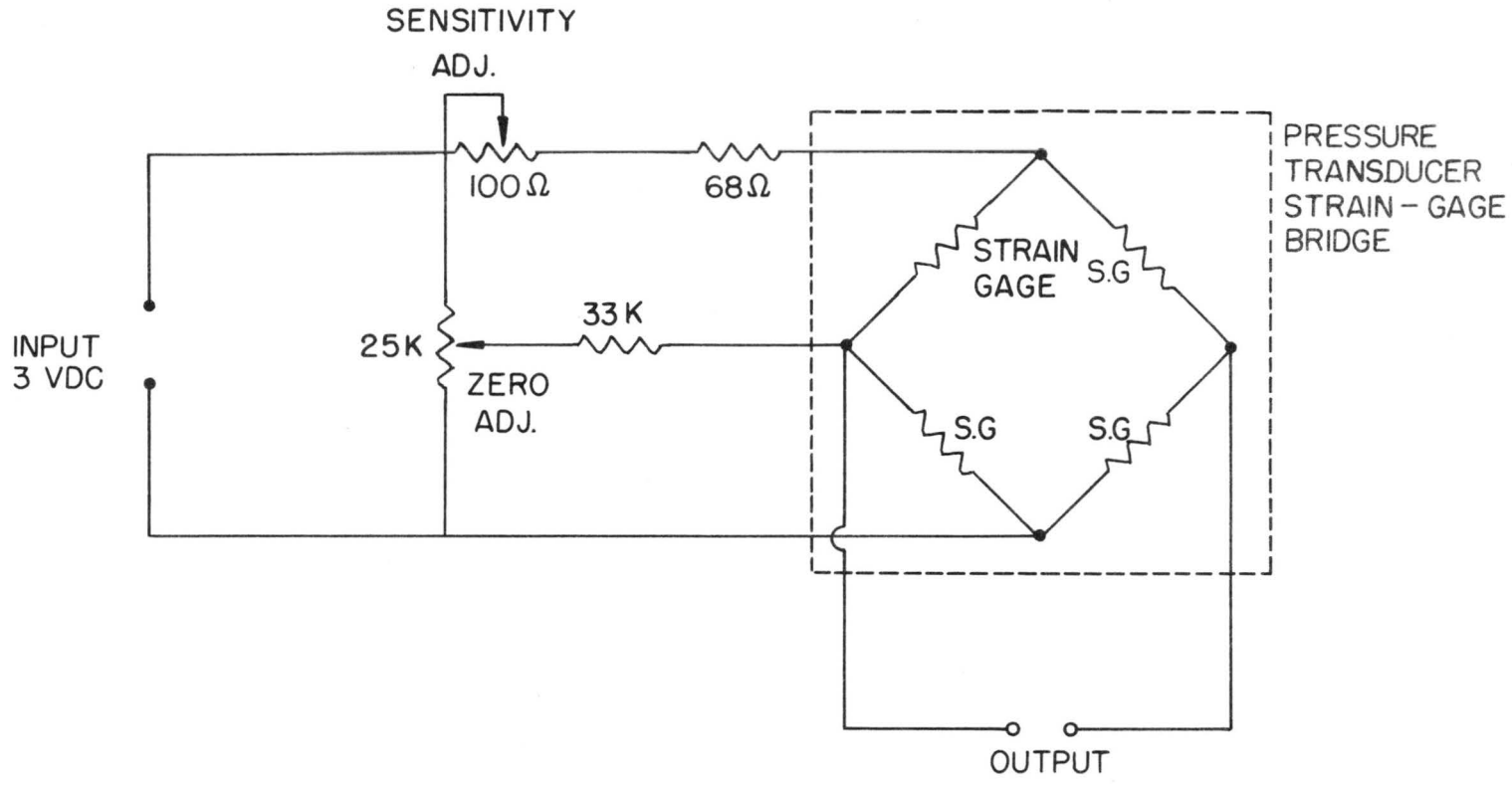

Figure 8. Pressure transducer strain-gage bridge with sensitivity and balance control circuit

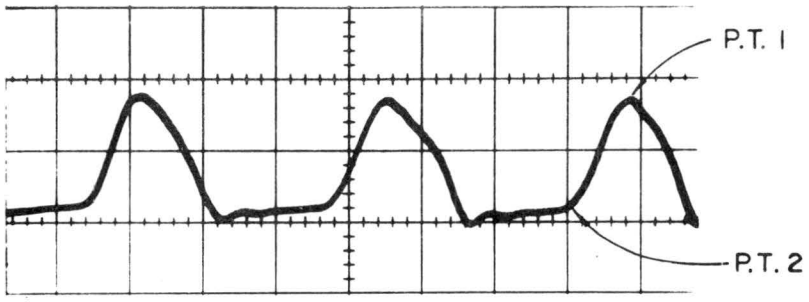

Time scale 20 msec/cm
Ampl. scale 1 mv/cm

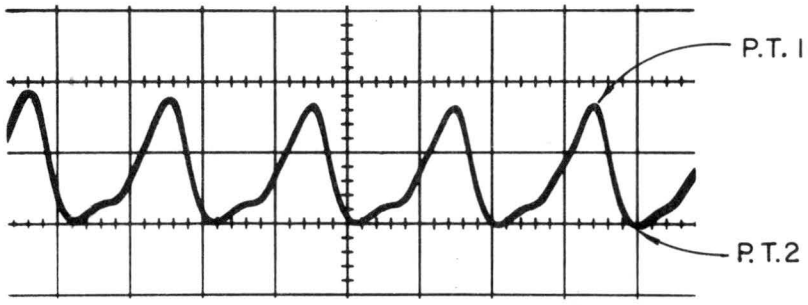

Time scale 10 msec/cm
Ampl. scale 1 mv/cm

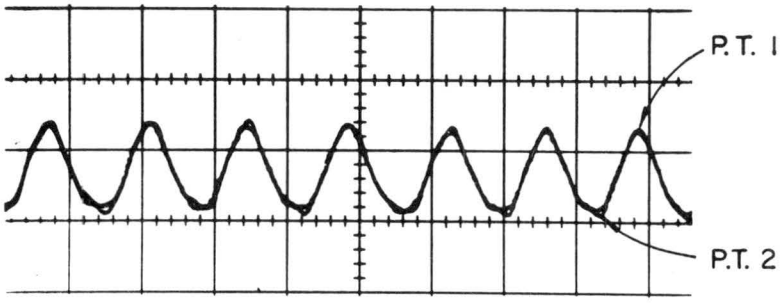

Time scale 5 msec/cm
Ampl. scale 1 mv/cm

Figure 9. Superimposed pressure transducer output wave form at low frequency

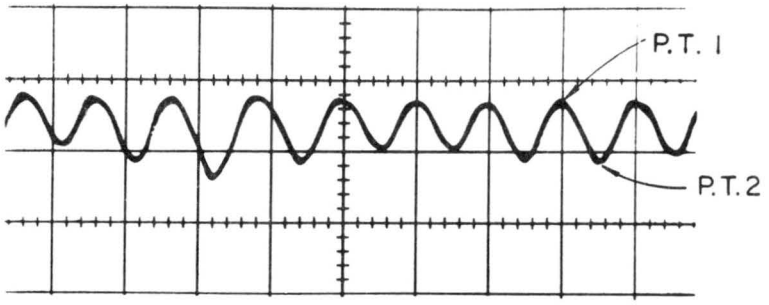

Time scale 5 msec/cm
Ampl. scale 1 mv/cm

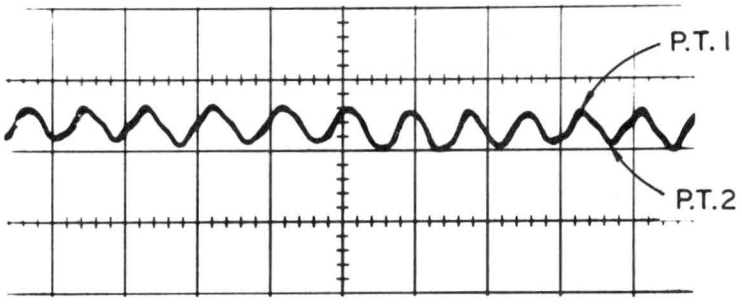

Time scale 5 msec/cm
Ampl. scale 1 mv/cm

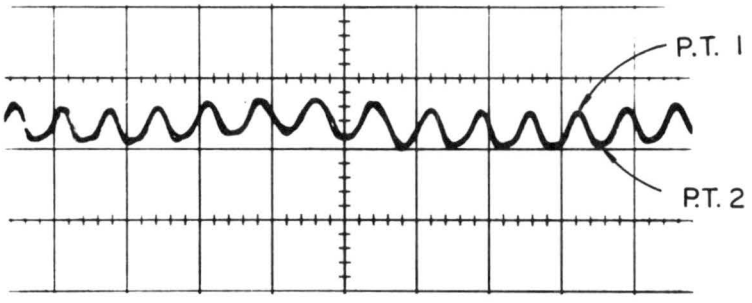

Time scale 5 msec/cm
Ampl. scale 1 mv/cm

Figure 10. Superimposed pressure transducer output wave form at high frequency

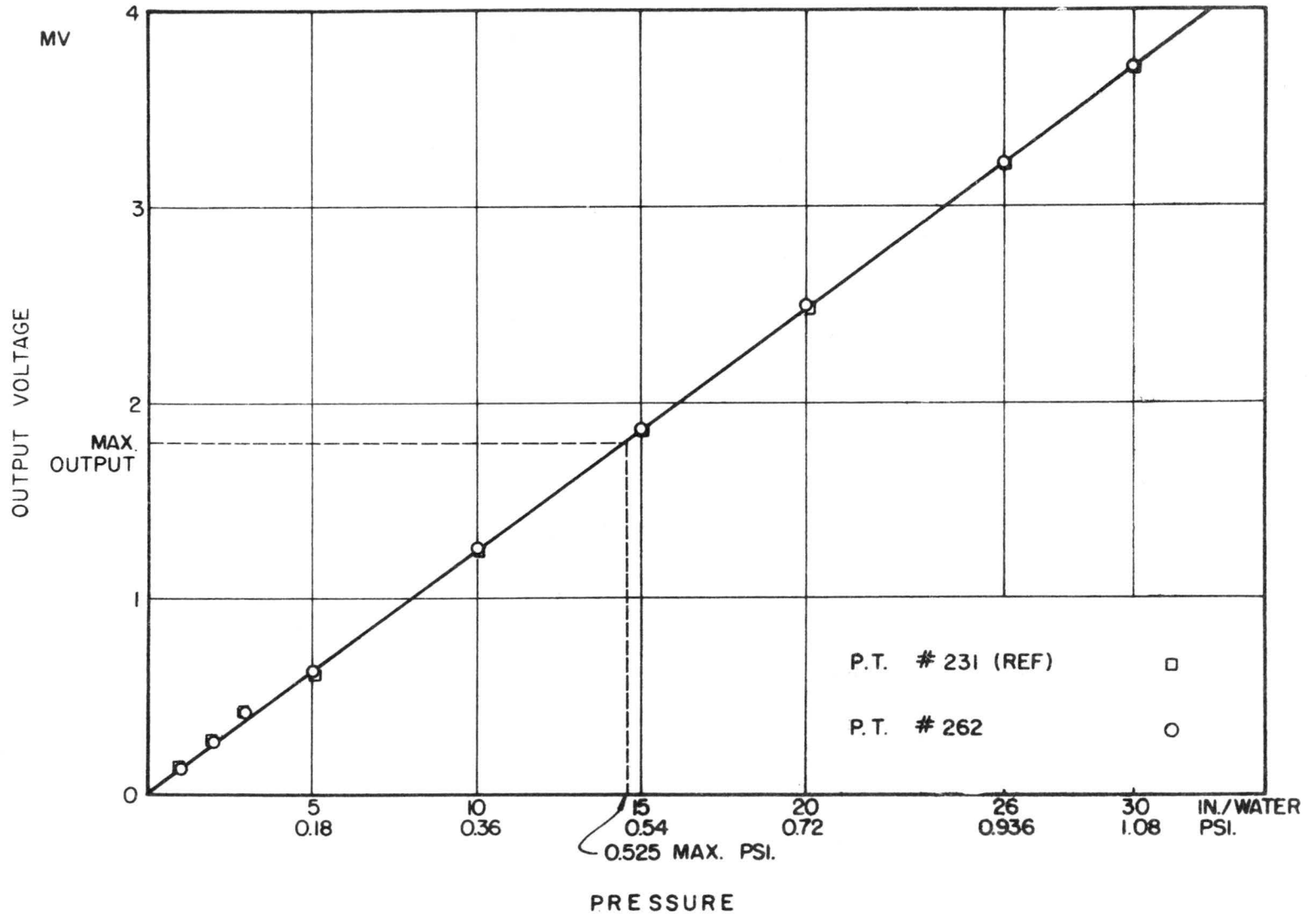

Figure 11. Calibration curves of pressure transducers

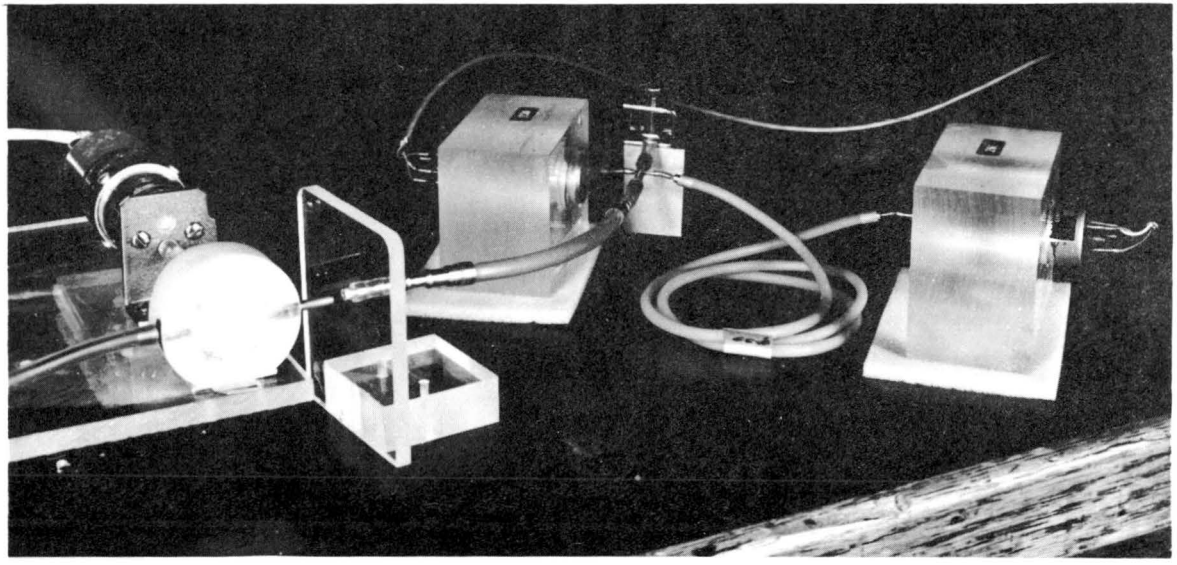

Figure 12. Pressure sensing system with the test tube

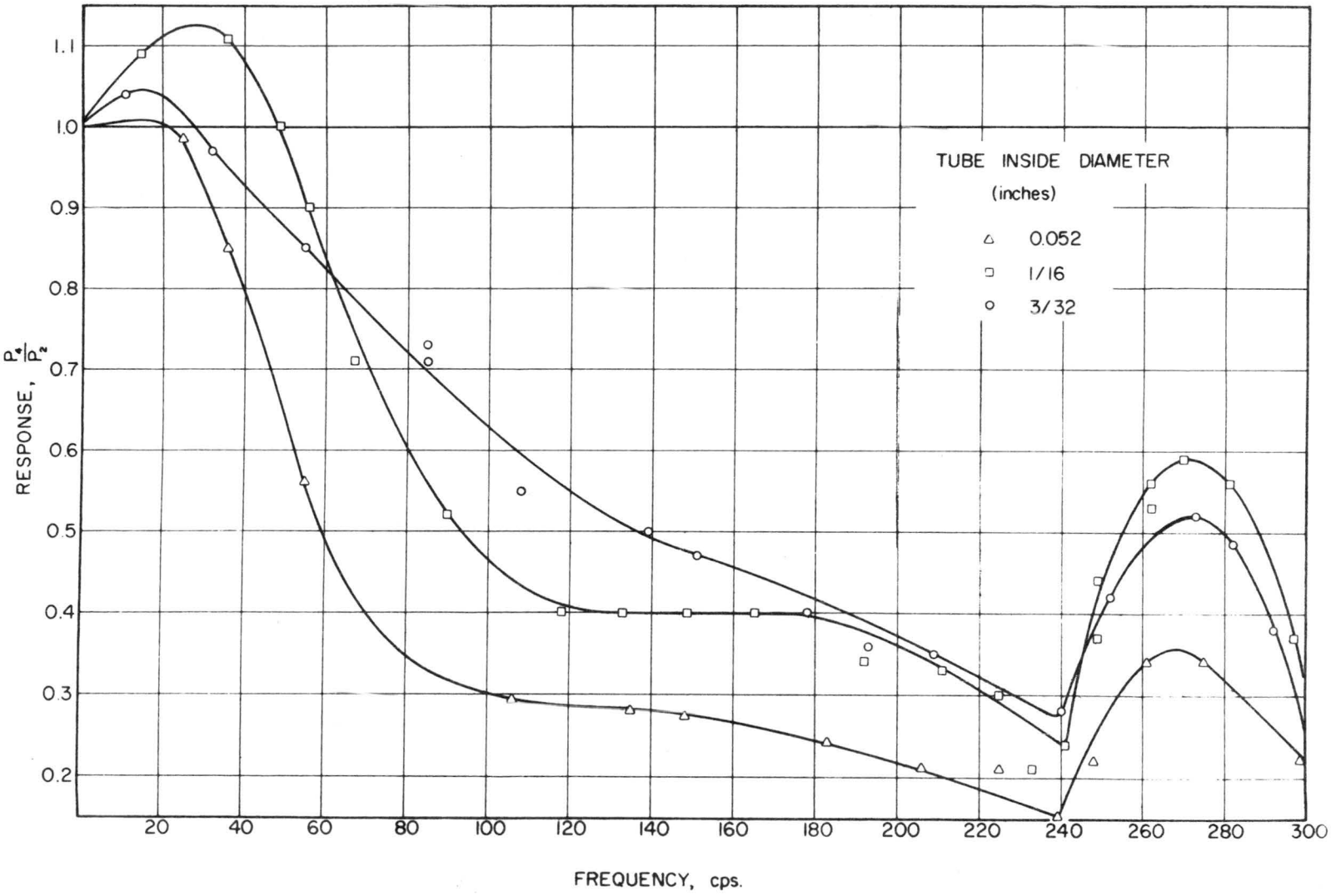

Figure 13. Response curves of 3-ft long flexible Tygon tubings to pulsating pressure variation without inlet restriction

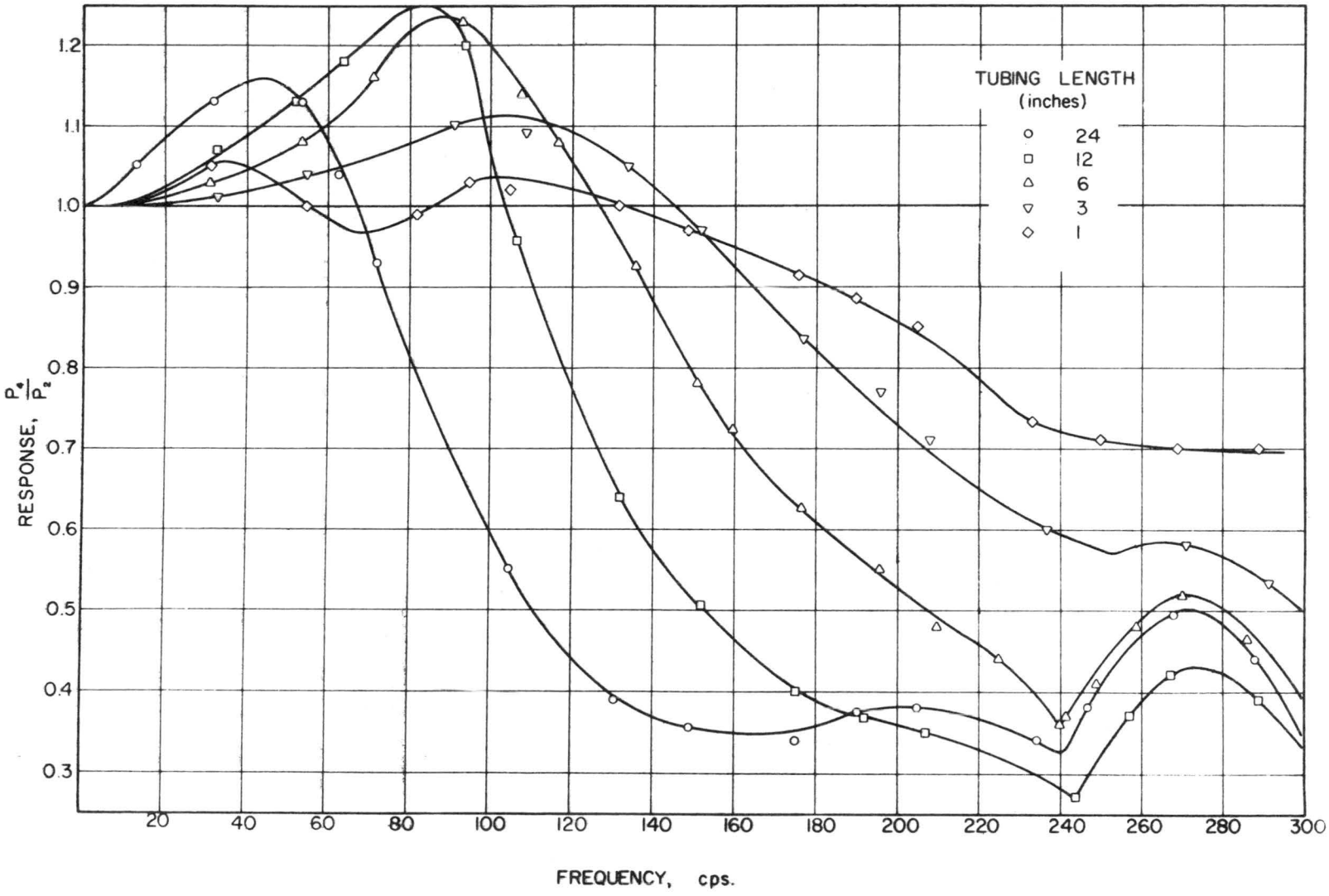

Figure 14. Response of 1/16-inch inside diameter flexible Tygon tubing to pulsating pressure variation

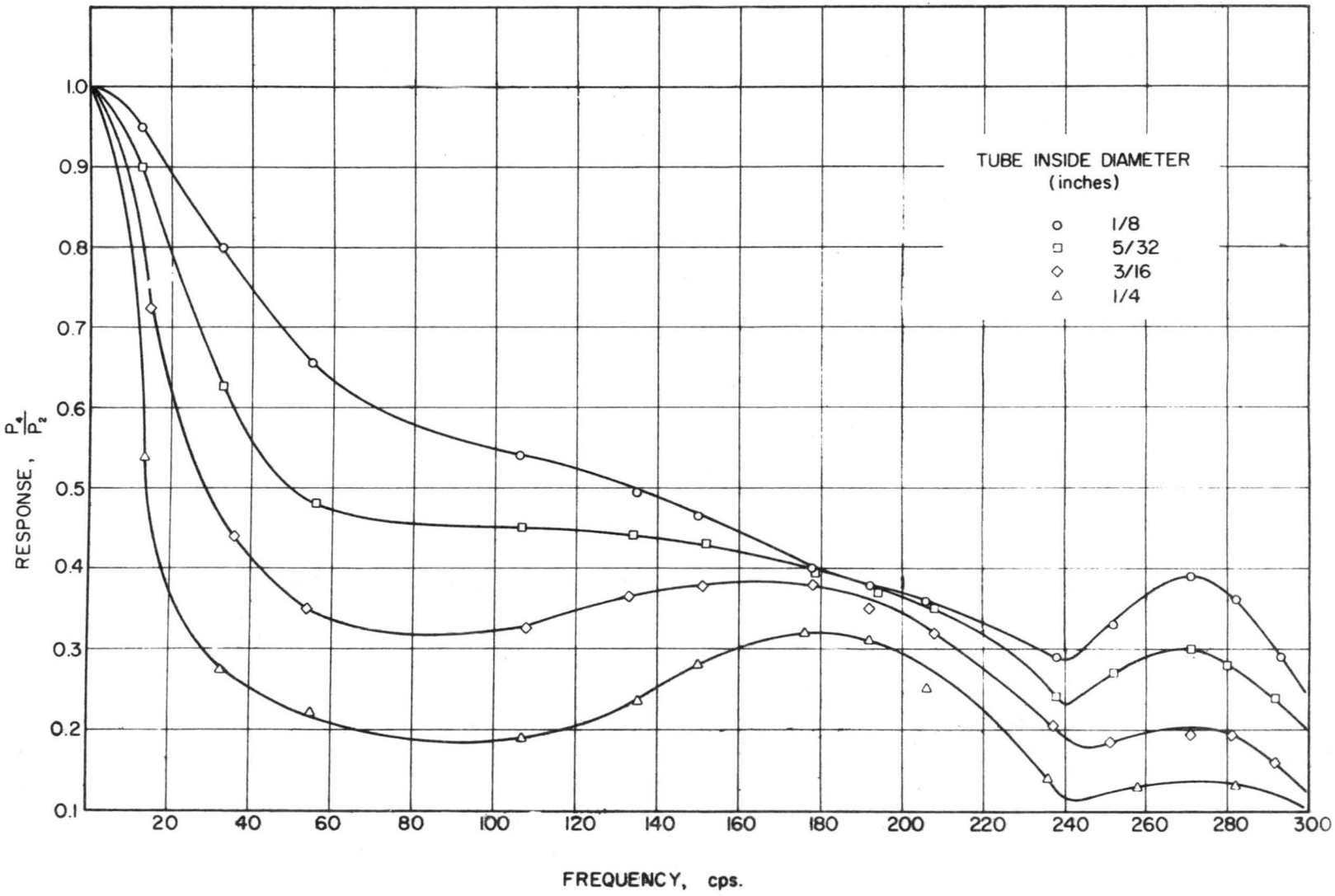

Figure 15. Response curves of 3 ft-long flexible Tygon tubings to pulsating pressure variation with inlet restriction

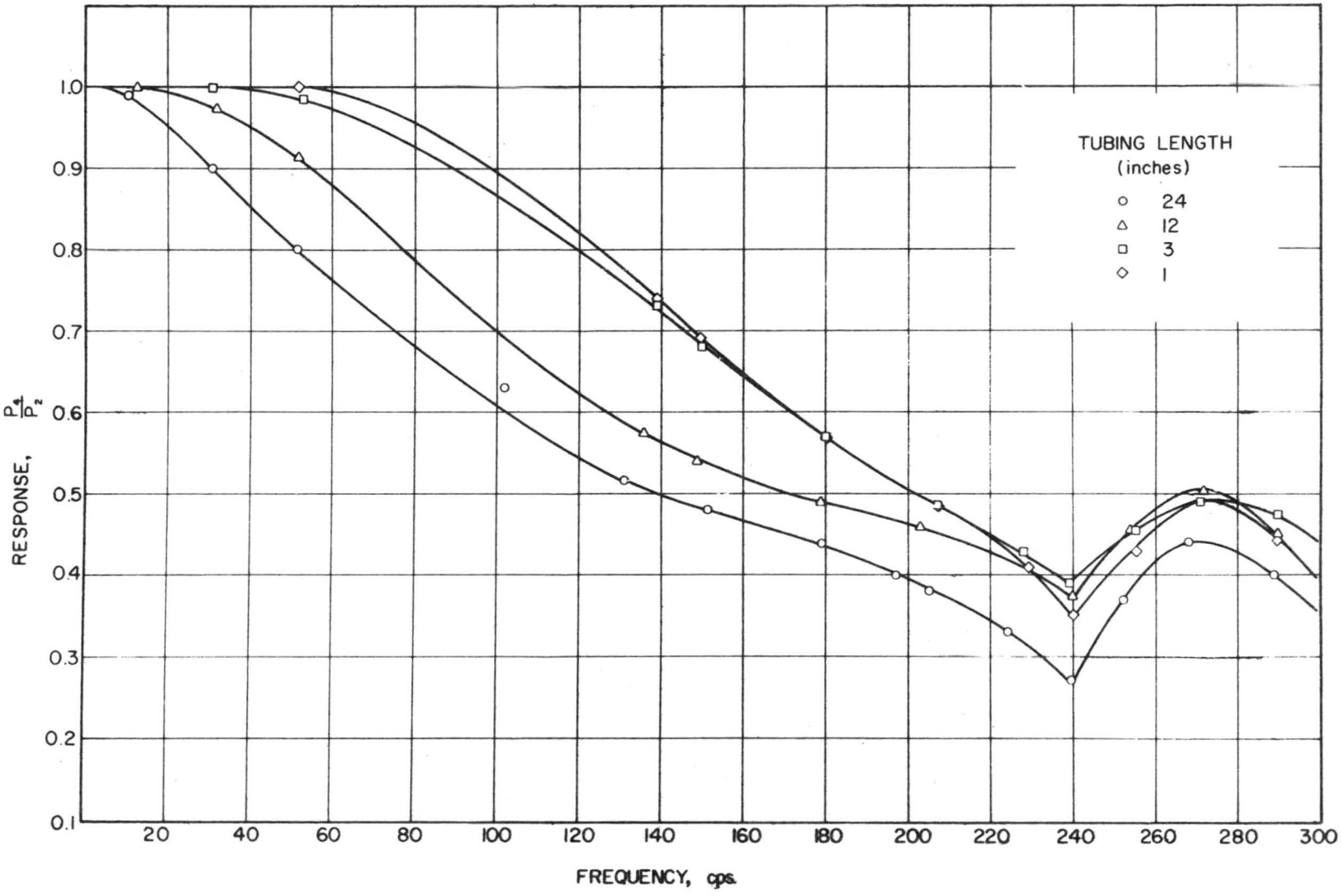

Figure 16. Response of 1/8-inch inside diameter flexible Tygon tubing to pulsating pressure variation

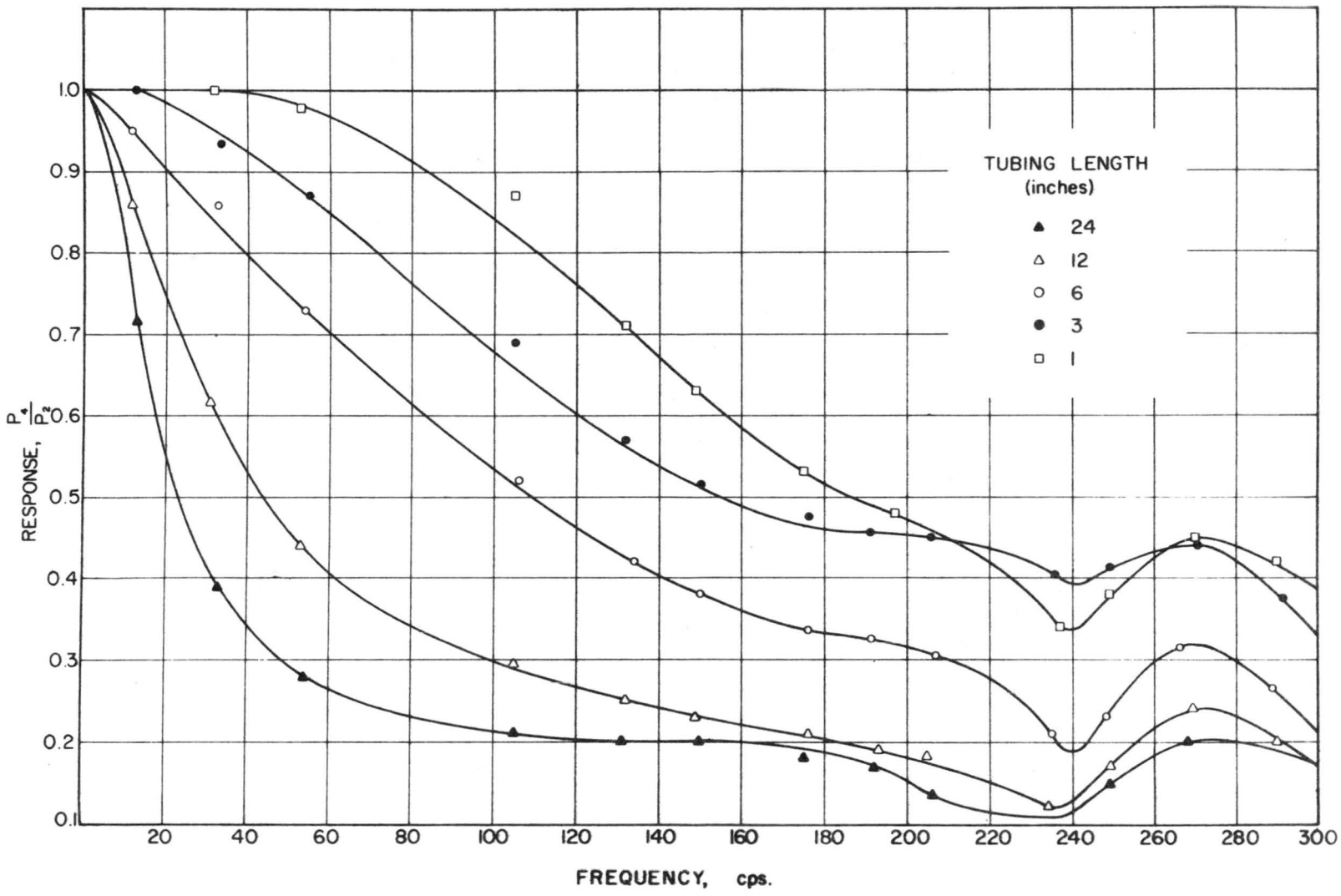

Figure 17. Response of 1/4-inch inside diameter flexible Tygon tubing to pulsating pressure variation

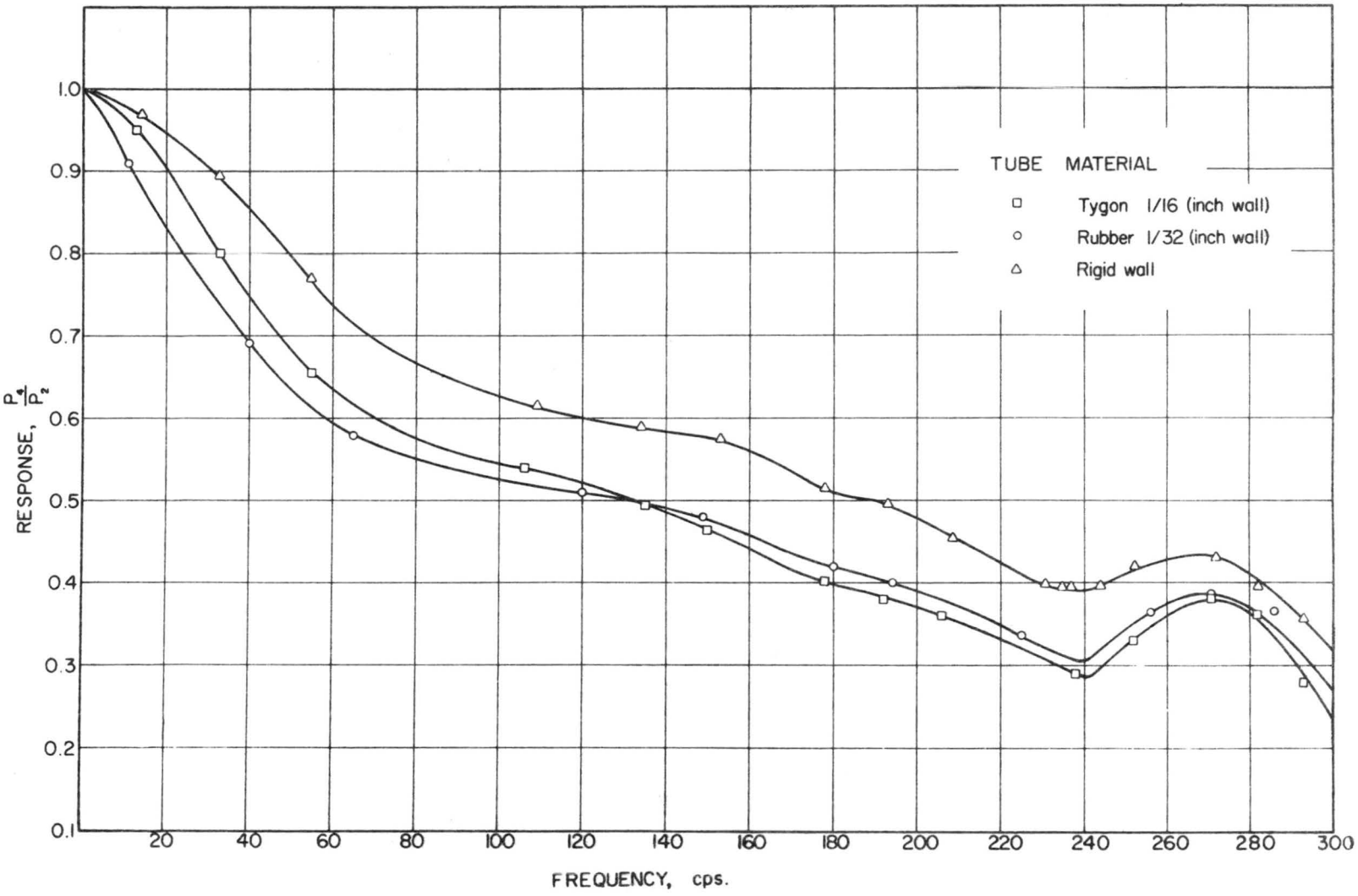

Figure 18. Response of 3-ft long, 1/8-inch inside diameter pressure lines to pulsating pressure variation with inlet restriction at 1/2-psi air pressure

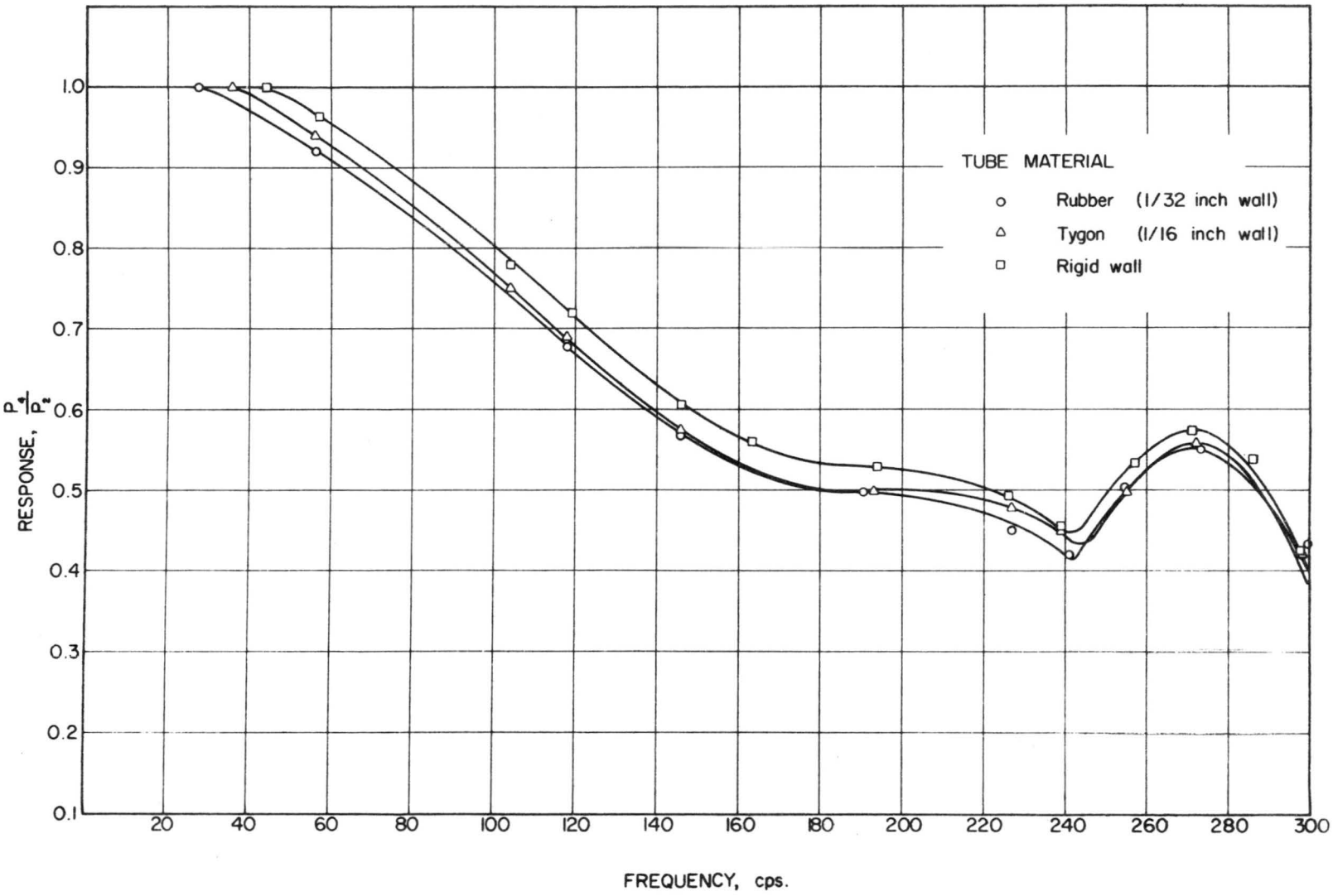

Figure 19. Response of 9 3/8-inch long, 1/8-inch inside diameter tubing to pulsating pressure variation at 1/2-psi air pressure

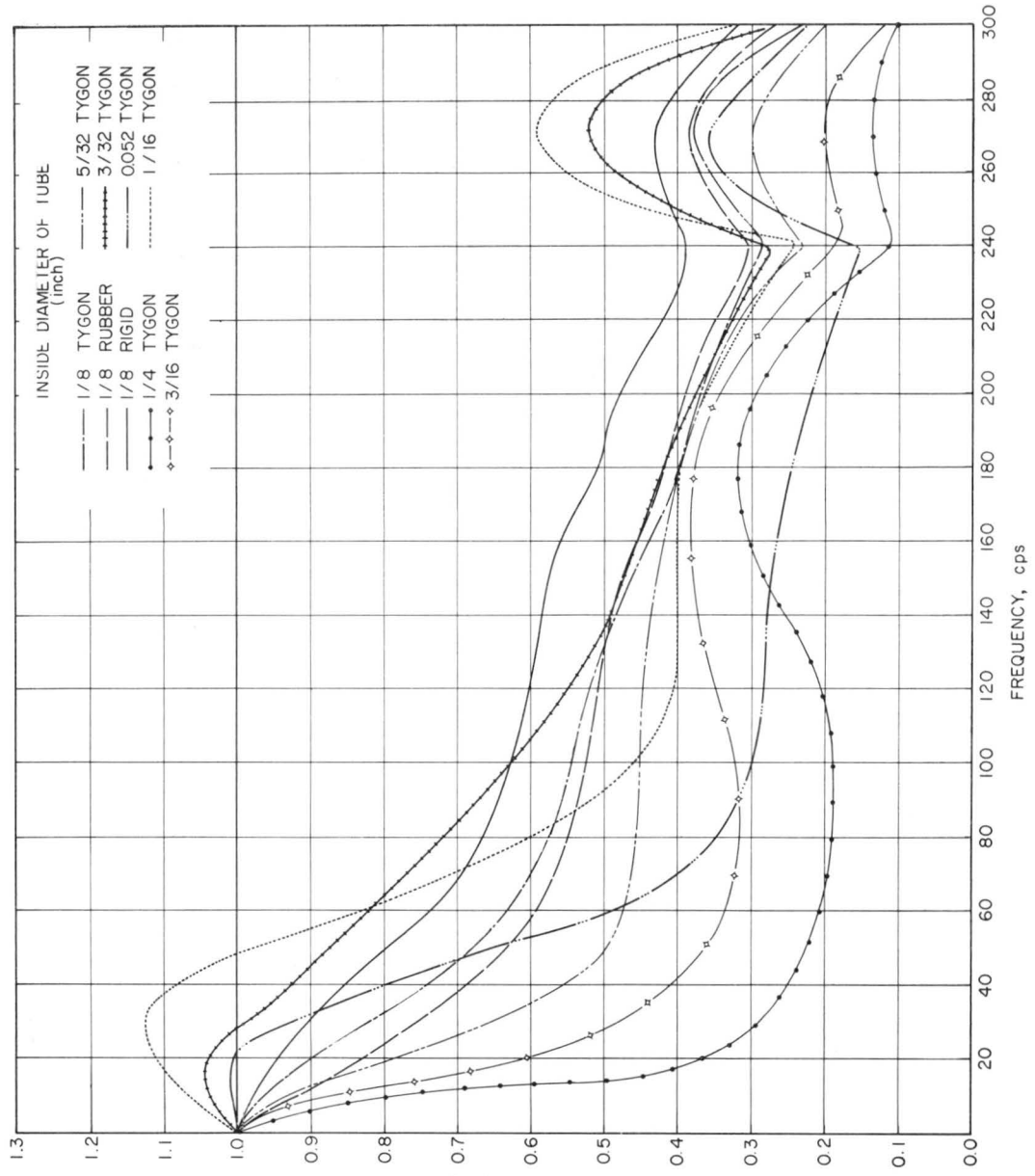

Figure 20. Response curves of 3-ft long Tygon (1/16-inch wall thickness) and rubber (1/32-inch wall thickness) pressure lines to pulsating pressure variation at 1/2-psi air pressure

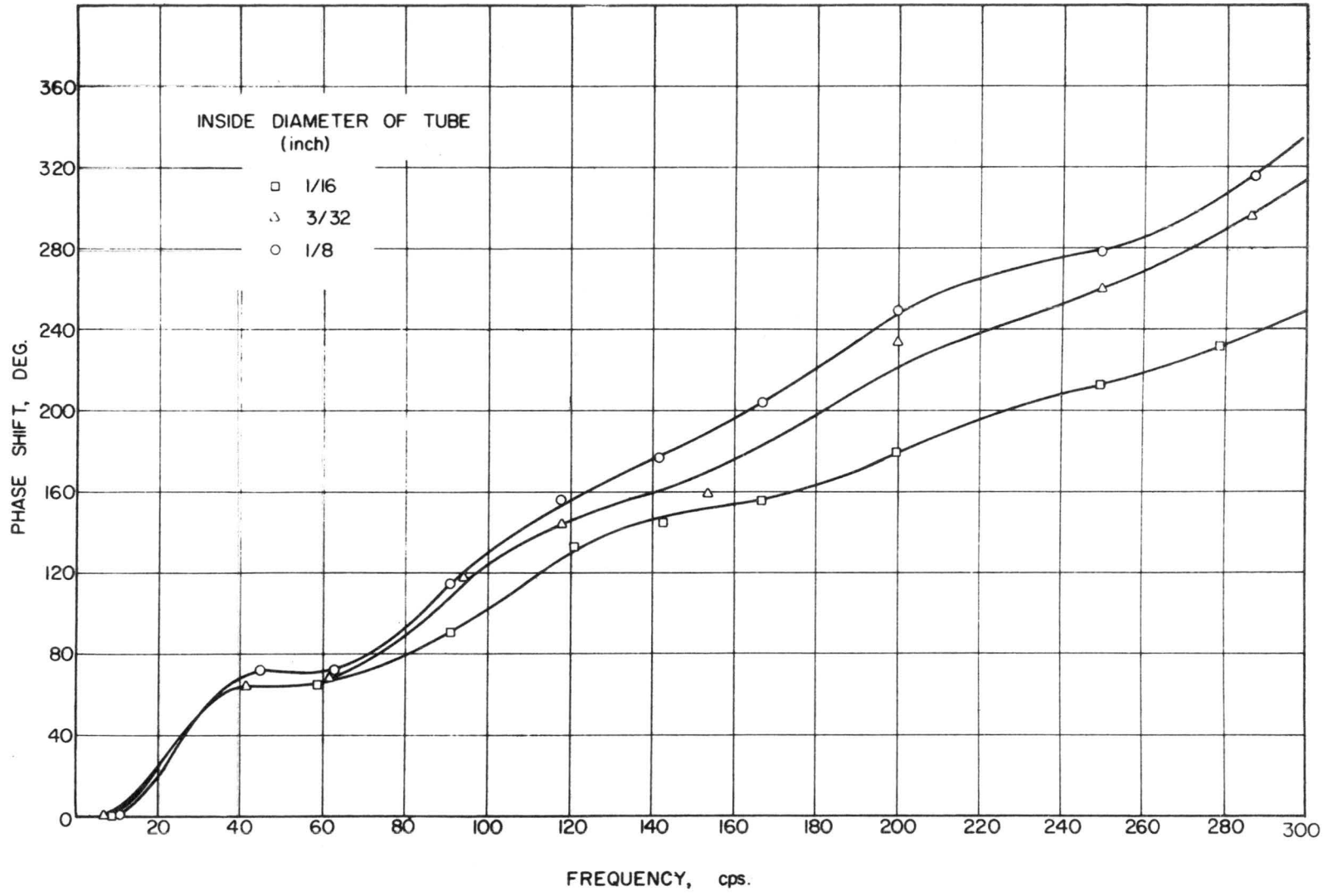

Figure 21. Lag curves for 3-ft Tygon tubings subjected to pulsating air pressure of 1/2 psi

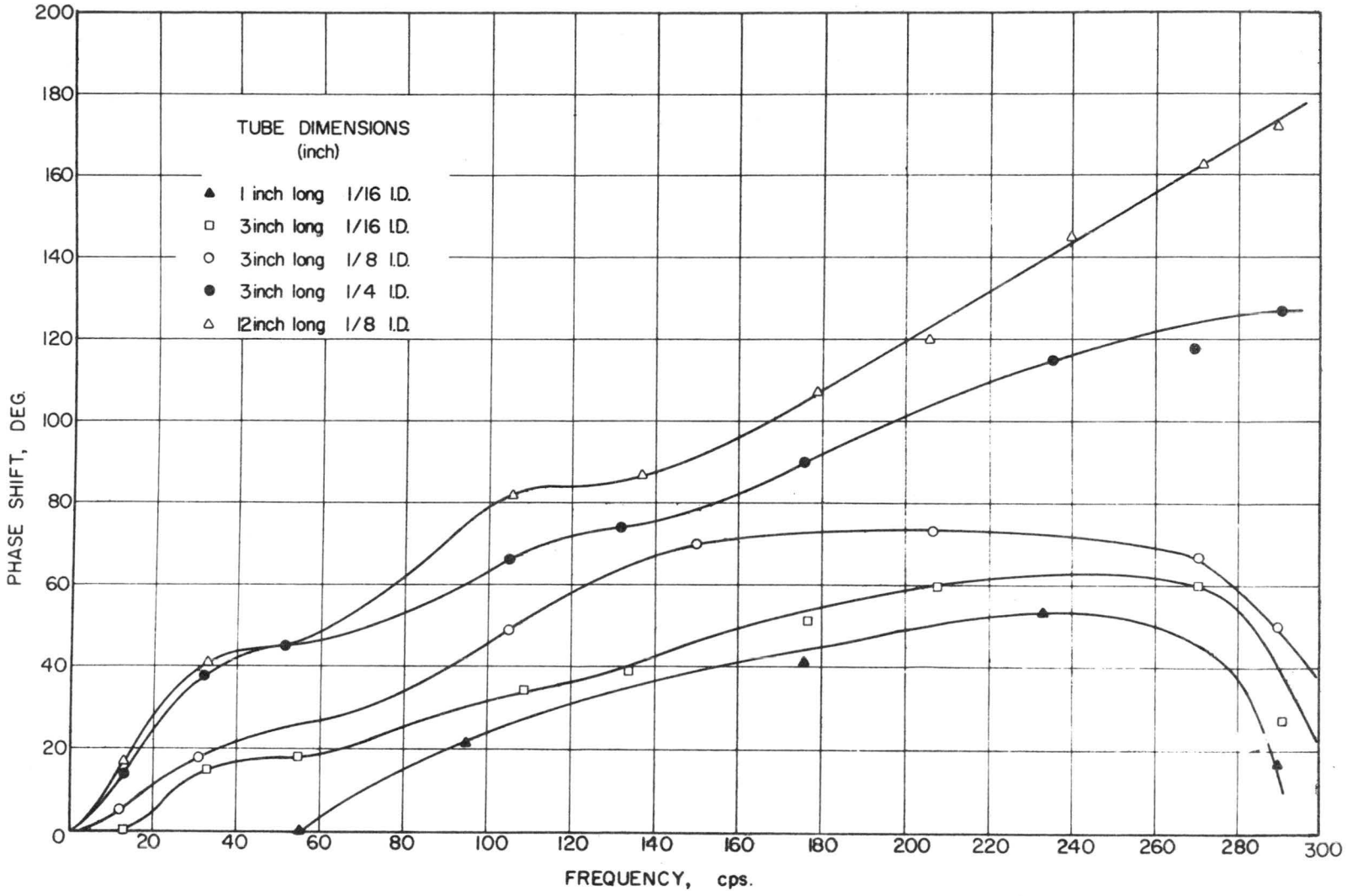

Figure 22. Phase shift for various length and inside diameter of Tygon tubings exposed to pulsating air pressure of 1/2 psi

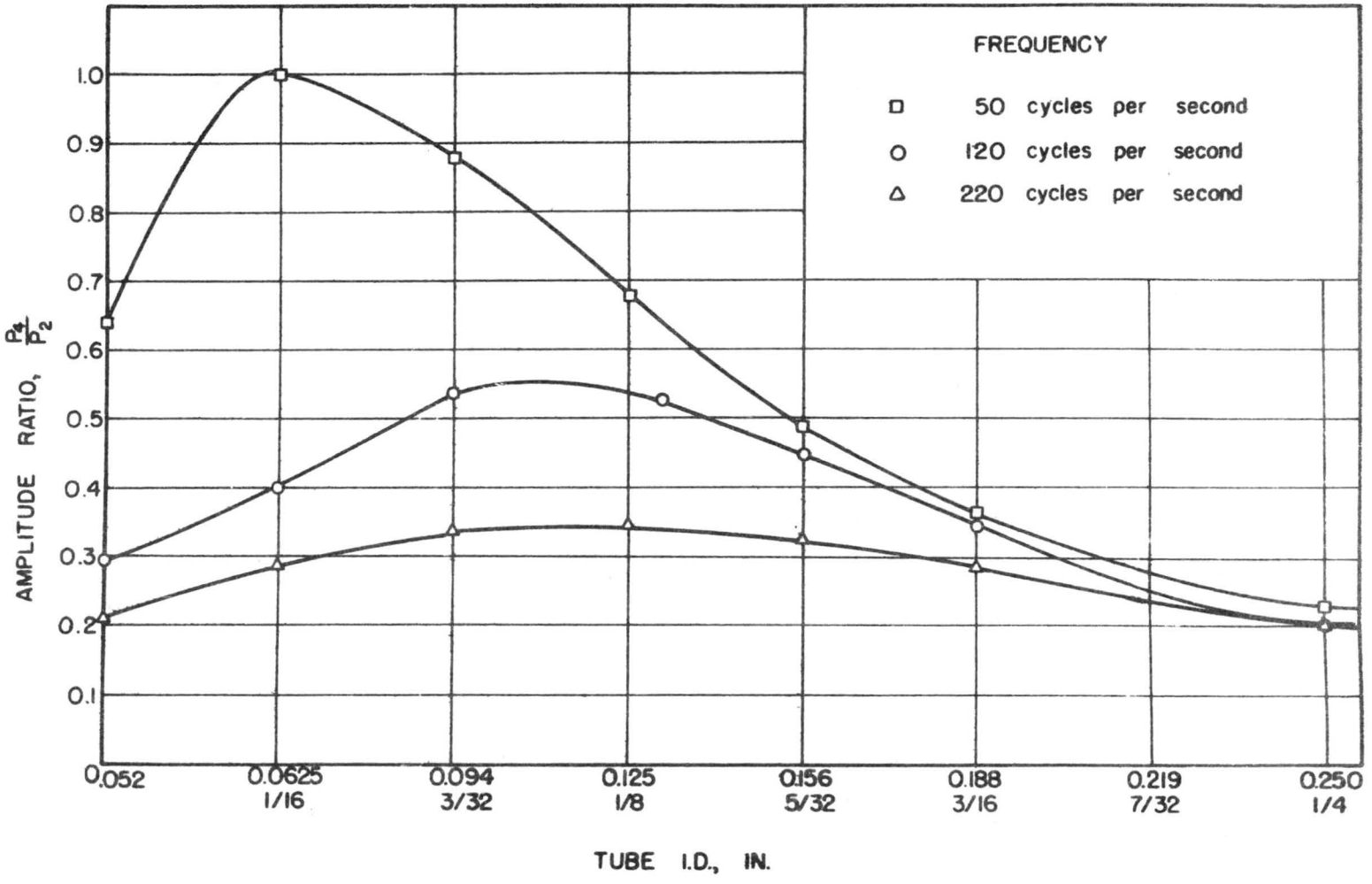

Figure 23. Pressure variation in 3-ft long Tygon tubings at various frequency

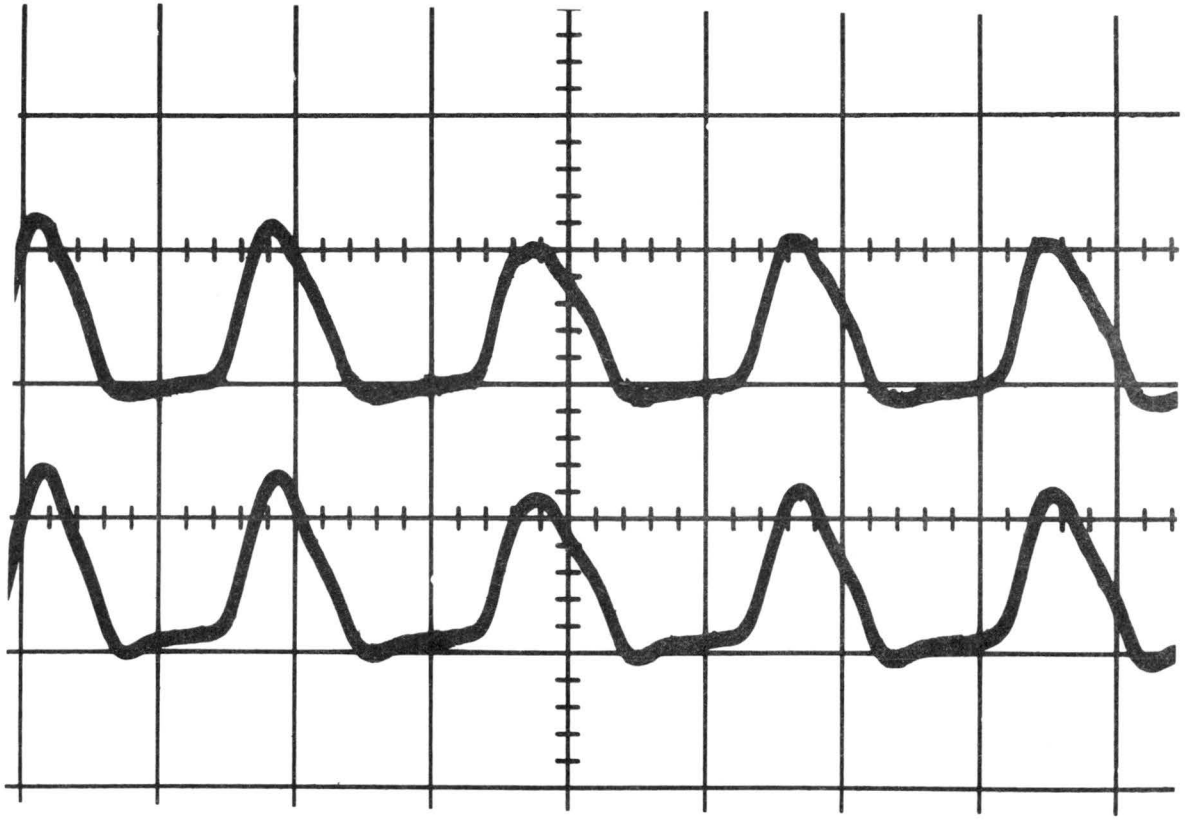

Figure 24. Pressure deviation in a 3-ft long, 3/32-inch diameter tubing

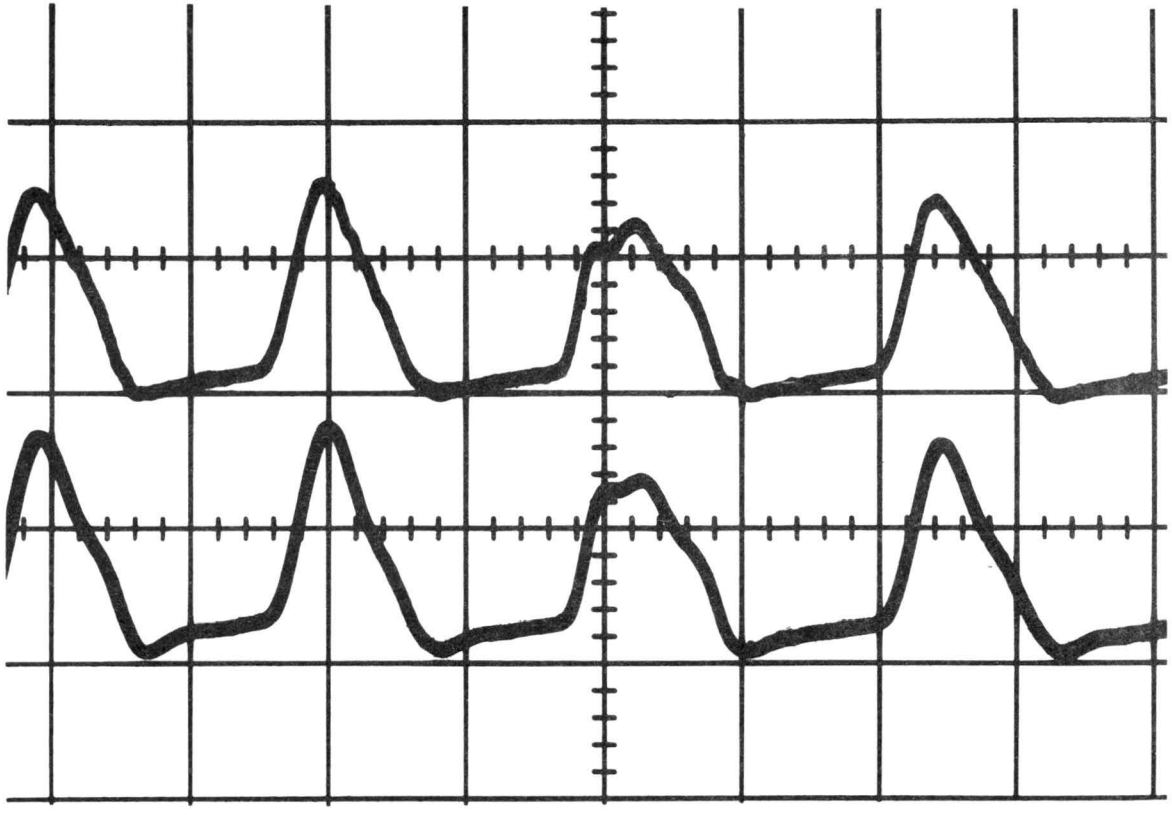

Figure 25. Pressure deviation in a 3-ft long, 1/16-inch inside diameter tubing

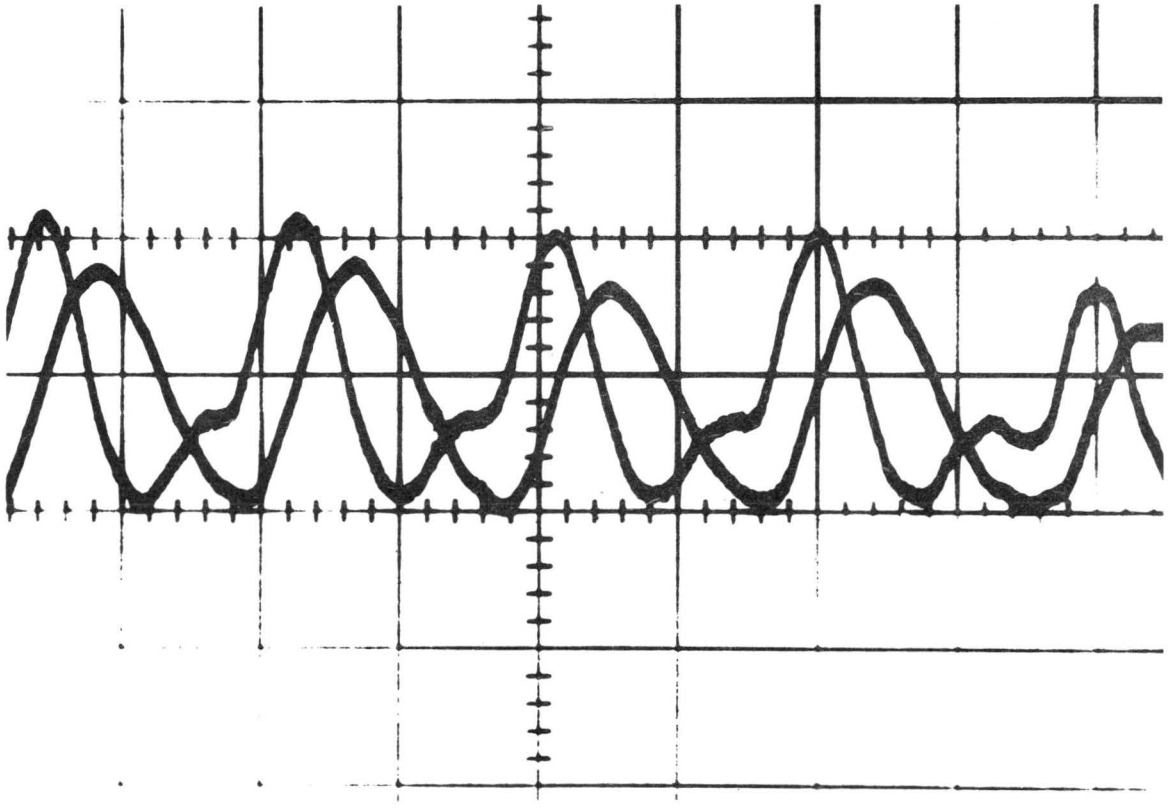

Figure 26. Pressure deviation in a 1-ft long, 1/16-inch inside diameter tubing

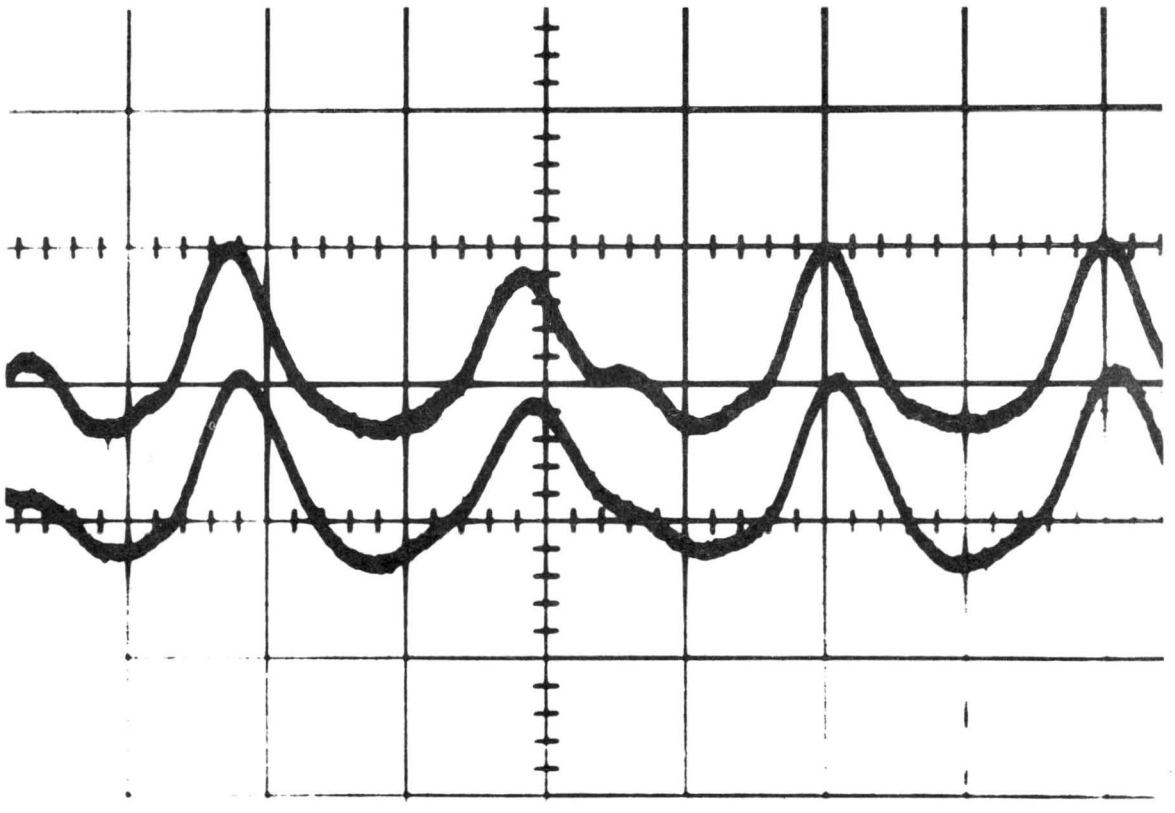

Figure 27. Pressure deviation in a 1-inch long, 1/16-inch inside diameter tubing

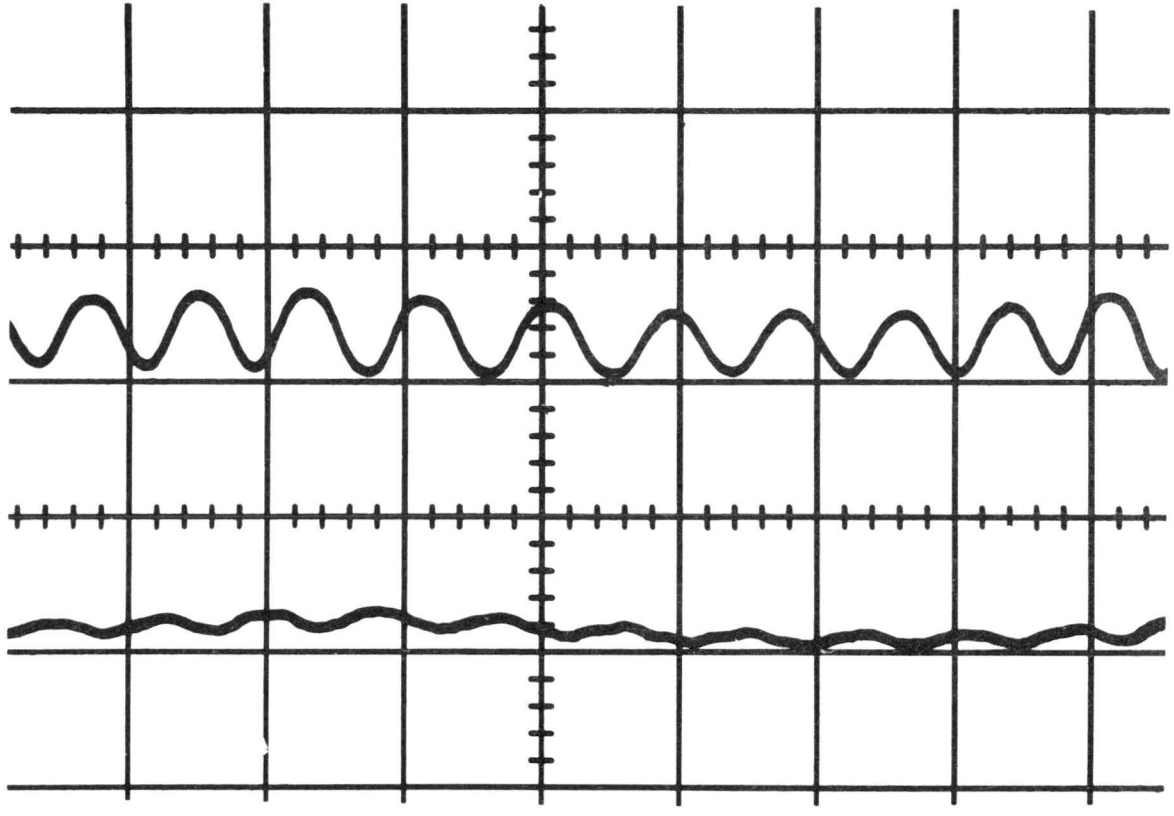

Figure 28. Pressure deviation in a 3-ft long, 1/16-inch inside diameter tubing

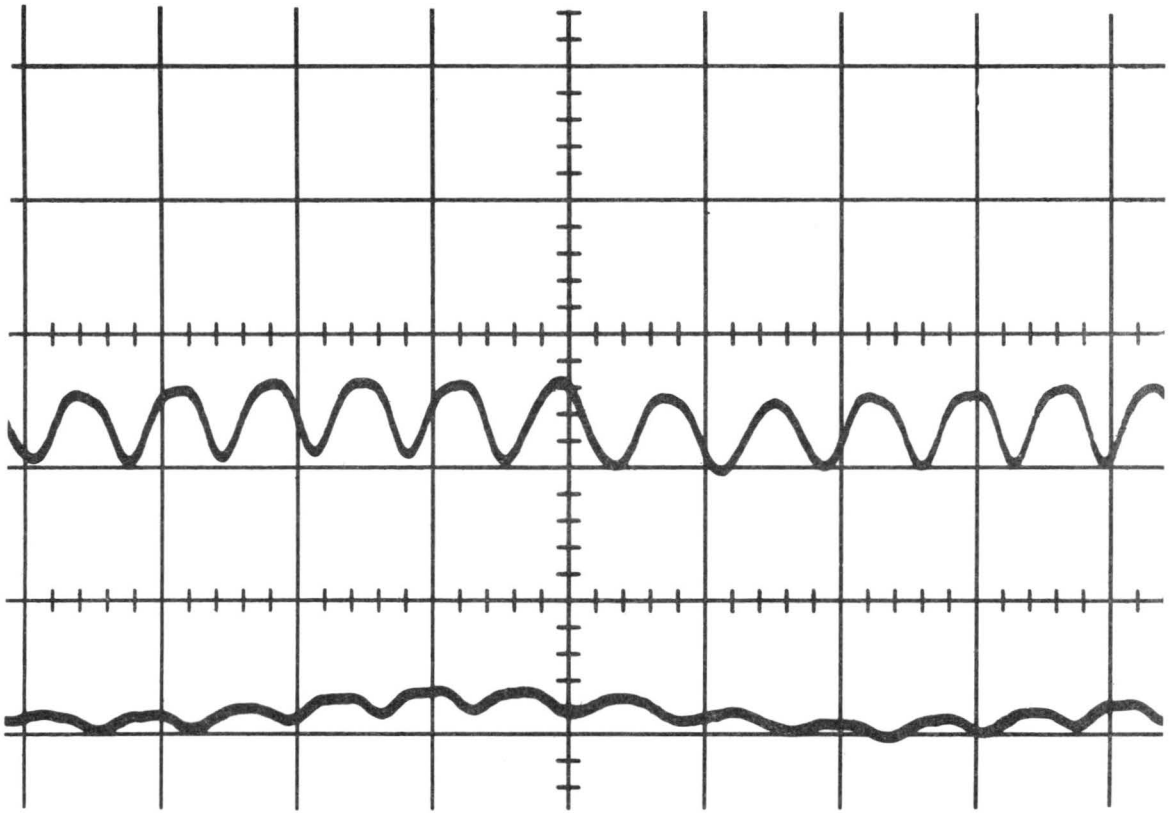

Figure 29. Pressure deviation in a 3-ft long, 1/16-inch inside diameter tubing

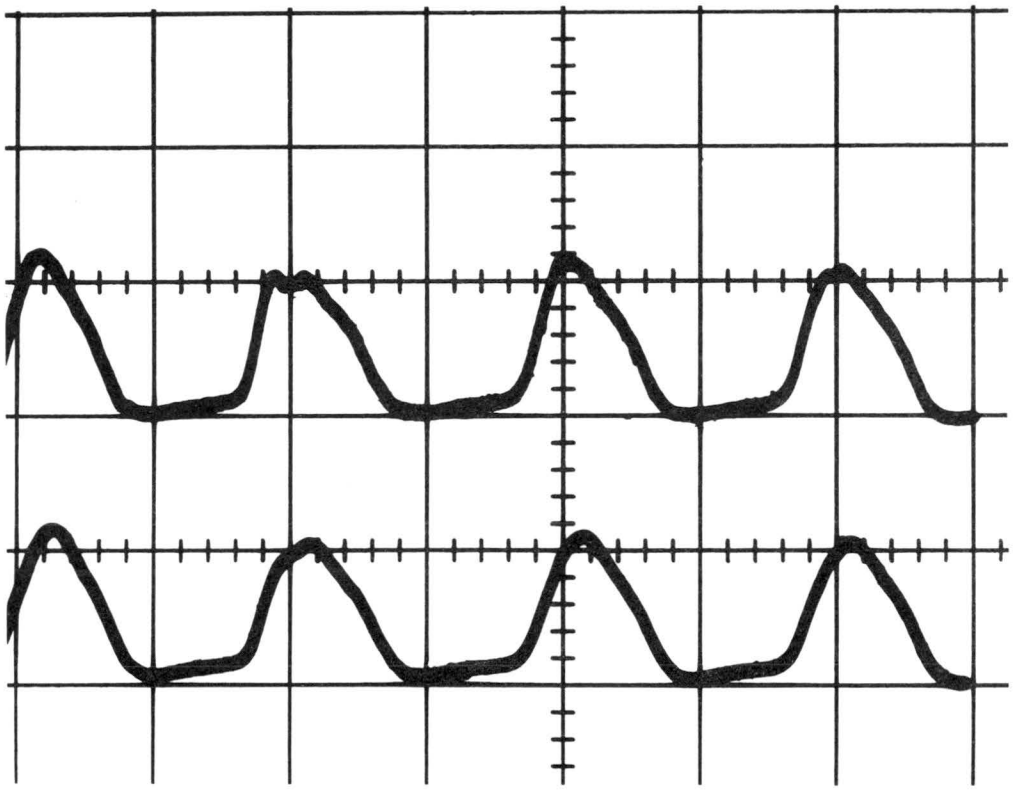

Figure 30. Pressure deviation in a 3-ft long, 1/8-inch inside diameter tubing

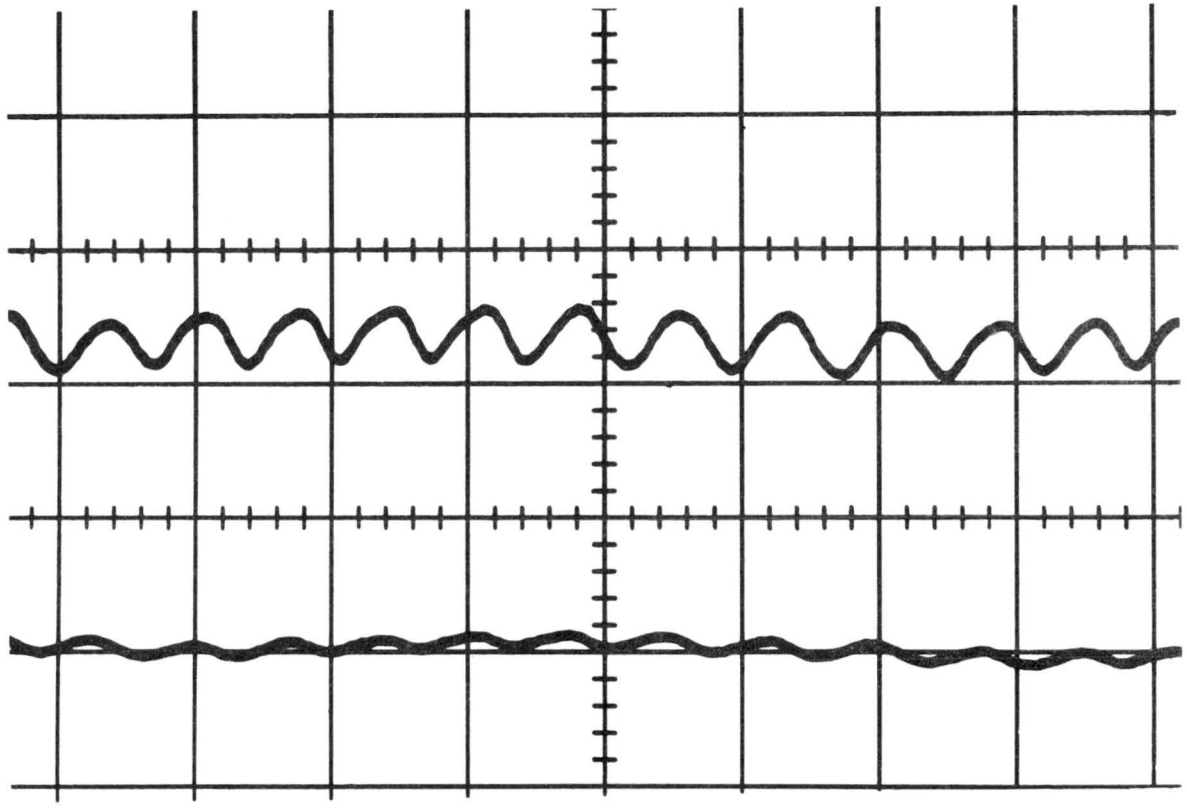

Figure 31. Pressure deviation in a 3-ft long, 1/8-inch inside diameter tubing

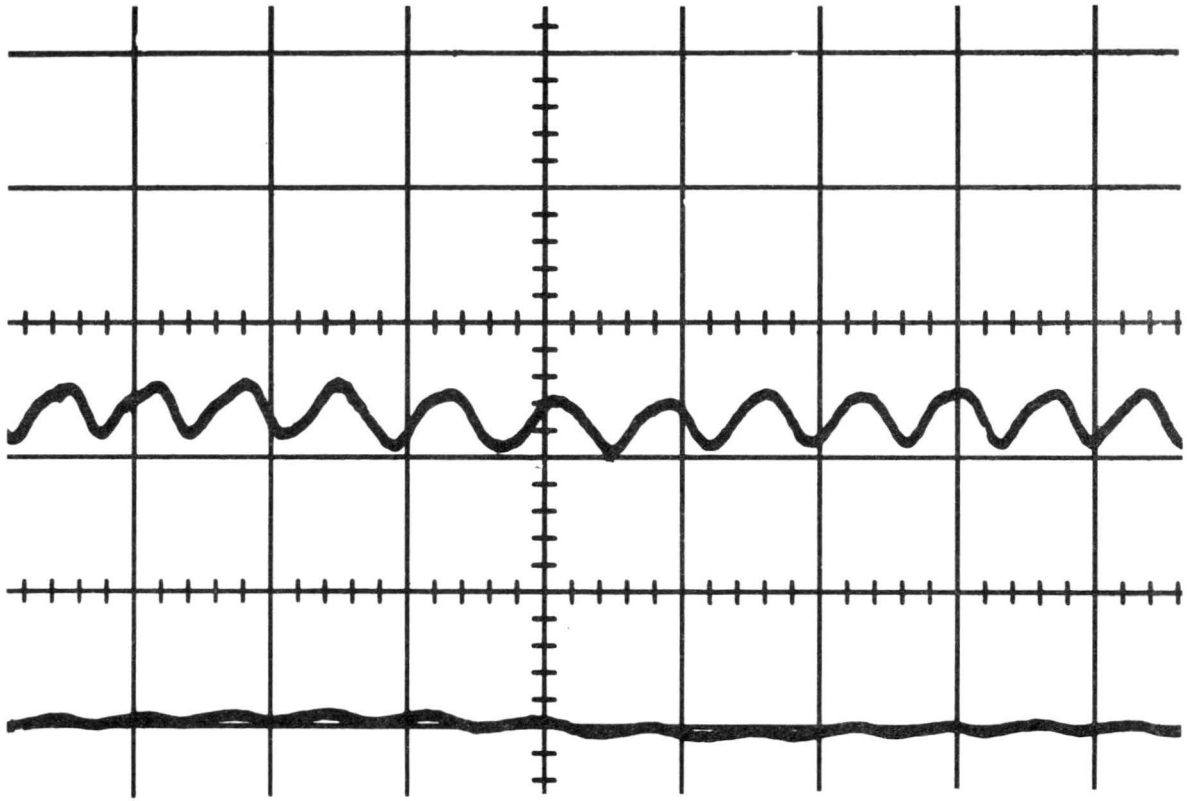

Figure 32. Pressure deviation in a 3-ft long, 5/32-inch inside diameter tubing

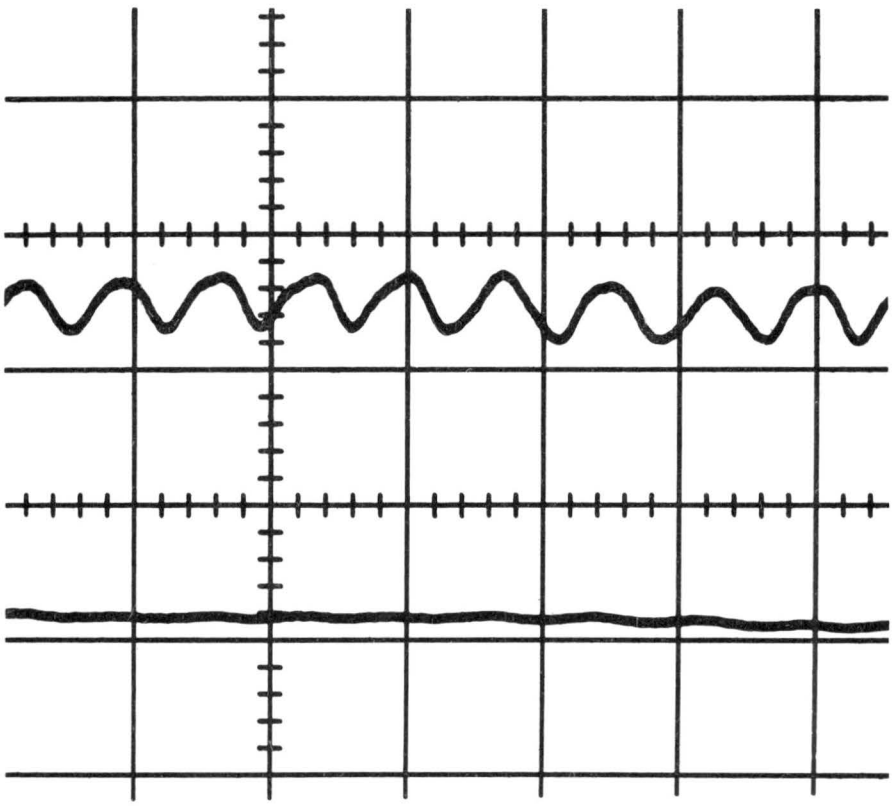

Figure 33. Pressure deviation in a 3-ft long 1/4-inch inside diameter tubing

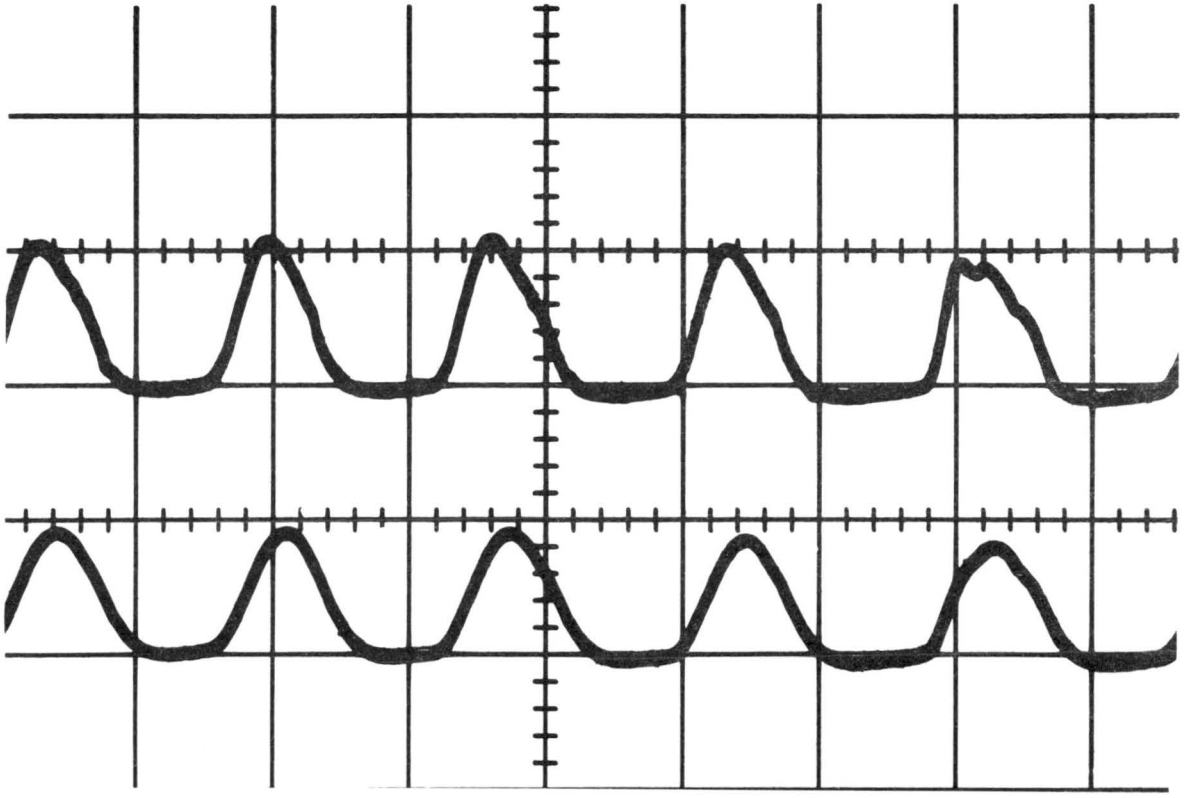

Figure 34. Phase shift in a 3-ft long, 5/32-inch inside diameter tubing

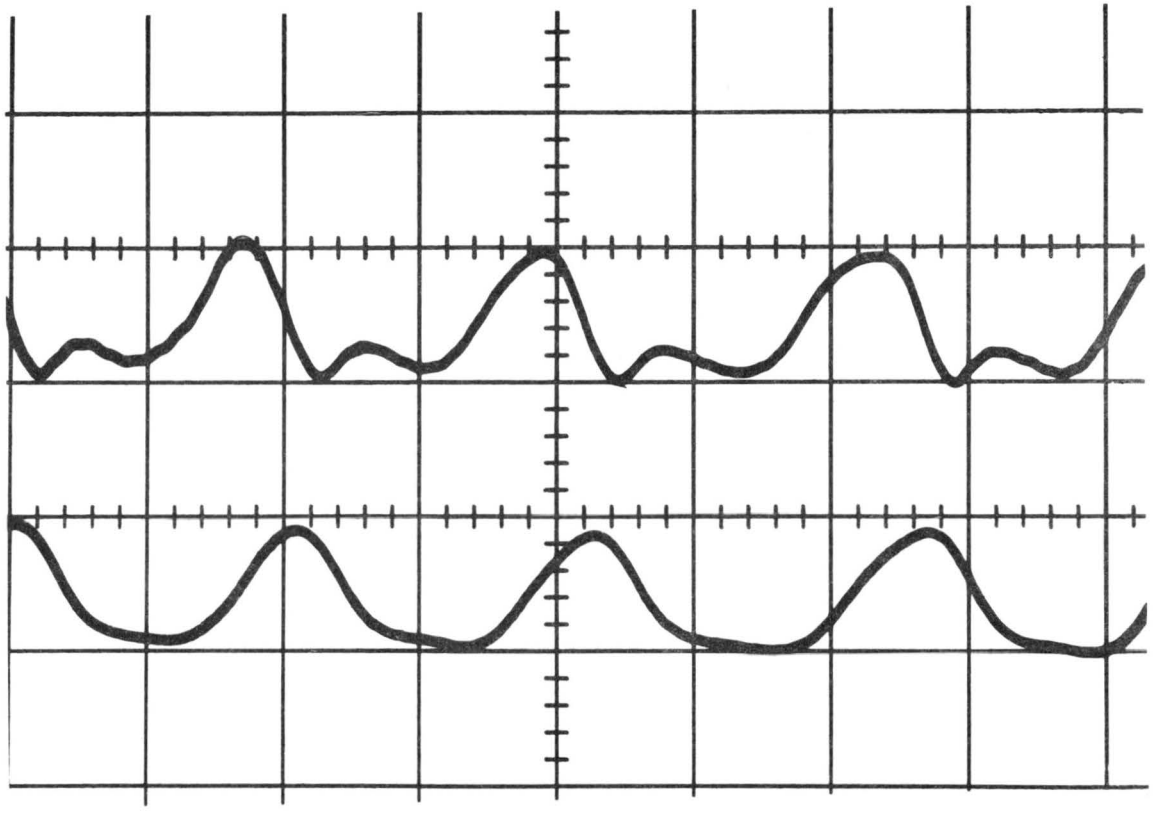

Figure 35. Phase shift in a 3-ft long, 3/32-inch inside diameter tubing

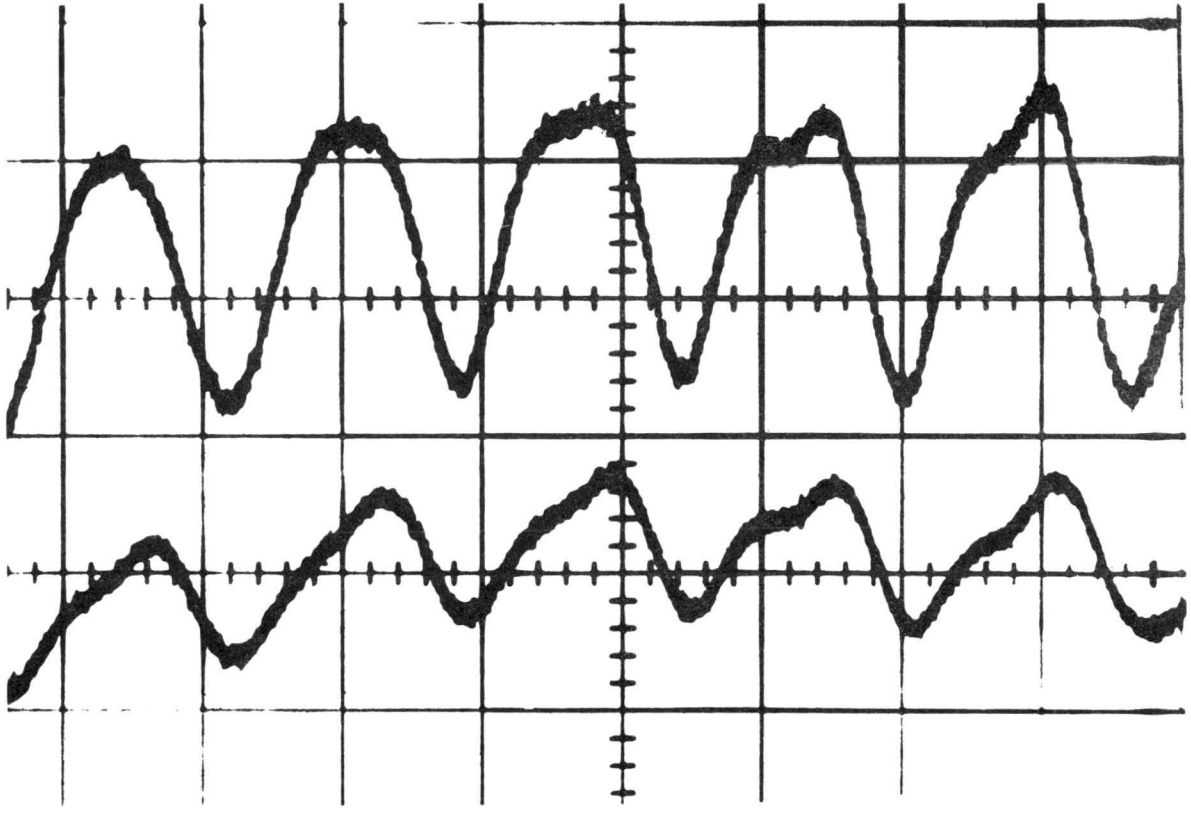

Figure 36. Phase shift in a 3-inch long, 1/16-inch inside diameter tubing

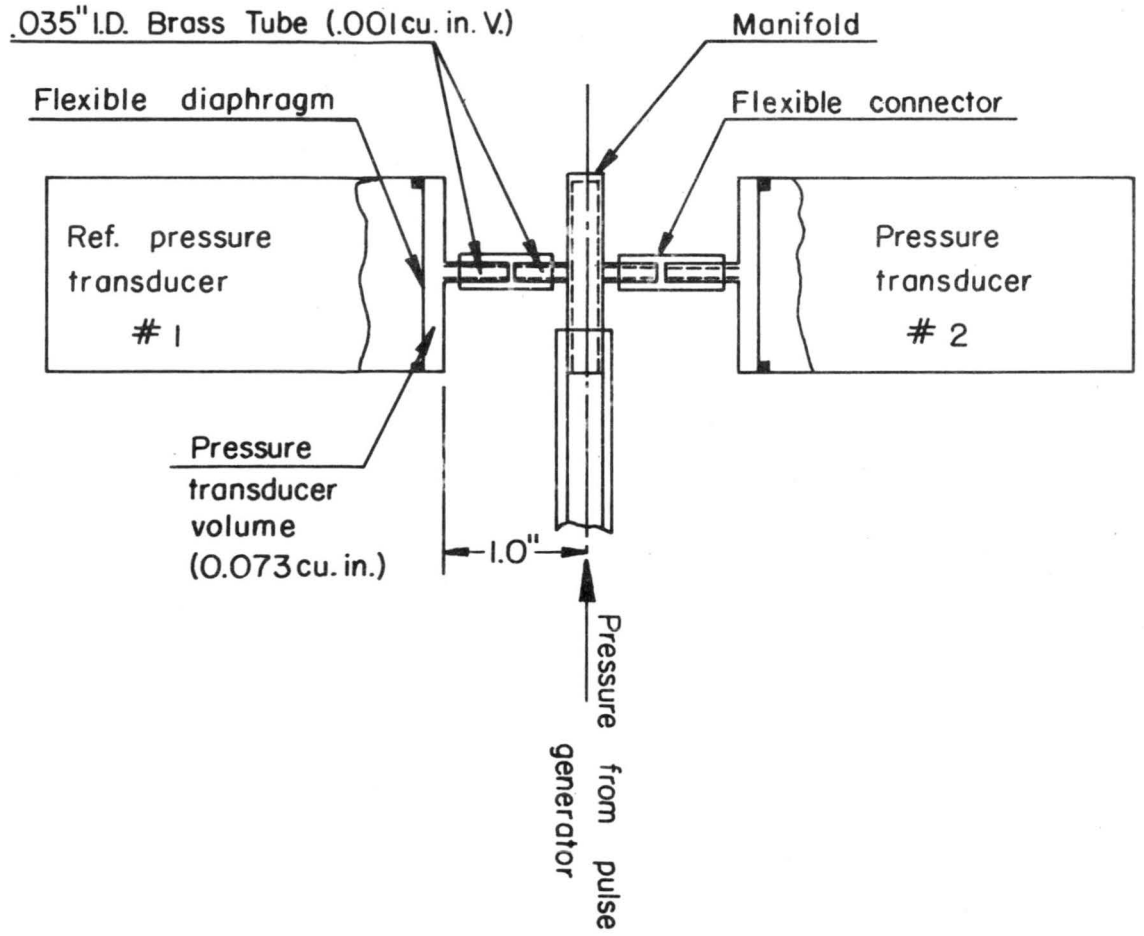

Figure 37. Connection of the manifold to the pressure transducers in calibration position

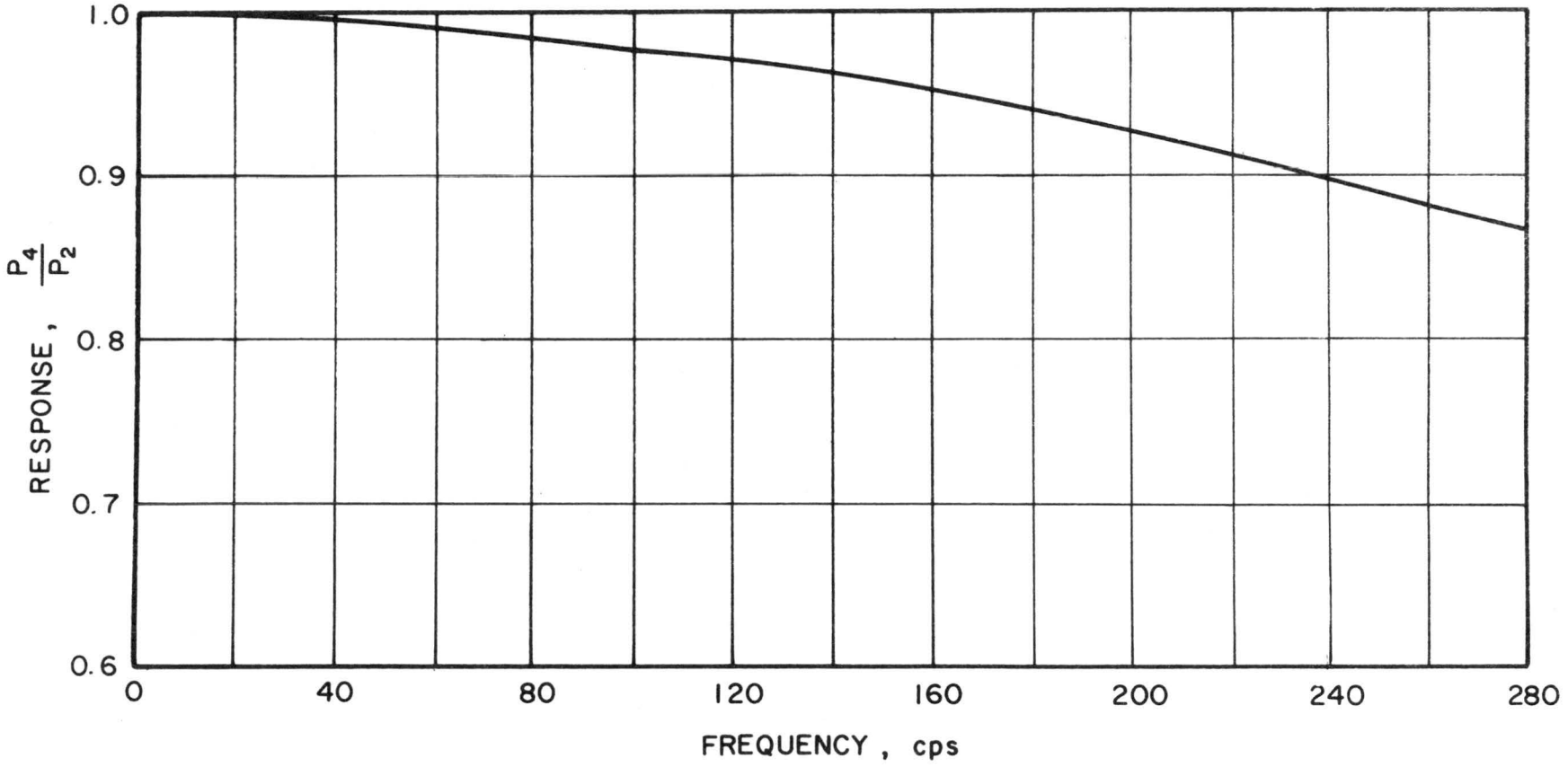

Figure 38. Response curve of the pressure system to pulsating pressure variation as calculated from equation A.2

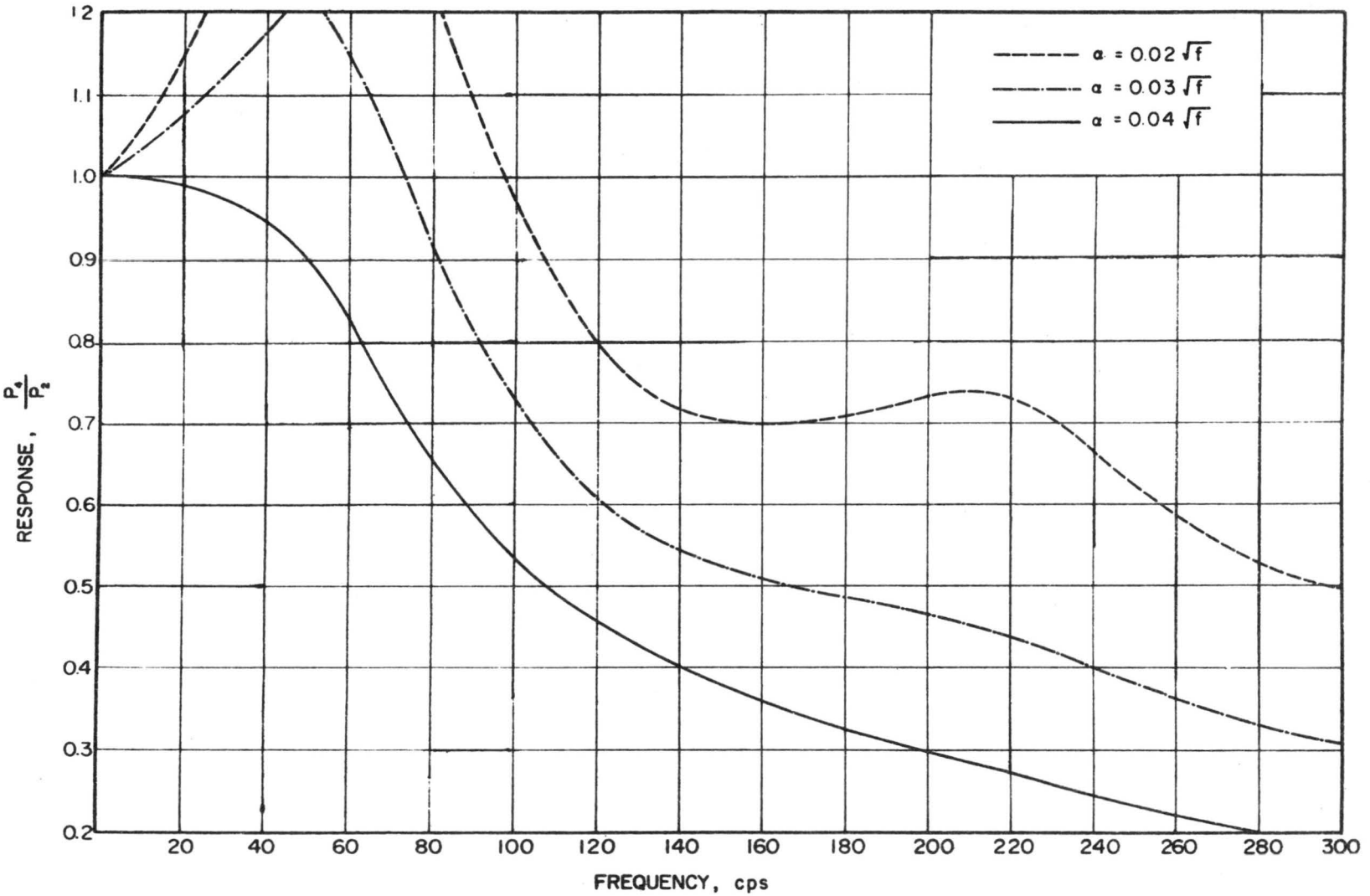

Figure 39. Response in the 1/16-inch inside diameter tubing with various attenuation constants as calculated from equation A.2

DOCUMENT CONTROL DATA - R&D

(Security classification of title, body of abstract and indexing annotation must be entered when the overall report is classified)

1. ORIGINATING ACTIVITY *(Corporate author)*

Fluid Mechanics Program, College of Engineering
Colorado State University, Fort Collins, Colorado

2a. REPORT SECURITY CLASSIFICATION

Unclassified

2b. GROUP

3. REPORT TITLE

DYNAMIC RESPONSE OF PRESSURE TRANSMISSION LINES TO PULSE INPUT

4. DESCRIPTIVE NOTES *(Type of report and inclusive dates)*

Technical Report

5. AUTHOR(S) *(Last name, first name, initial)*

Gorove, Arpad and J. E. Cermak

6. REPORT DATE
June 1967

7a. TOTAL NO. OF PAGES
93

7b. NO. OF REFS
21

8a. CONTRACT OR GRANT NO.
DA AMC 28-043-65-G20

b. PROJECT NO. 2246

c.

d.

9a. ORIGINATOR'S REPORT NUMBER(S)

CER66-67AP51

9b. OTHER REPORT NO(S) *(Any other numbers that may be assigned this report)*

10. AVAILABILITY/LIMITATION NOTICES

Distribution of This Document is Unlimited

11. SUPPLEMENTARY NOTES

12. SPONSORING MILITARY ACTIVITY

U. S. Army Materiel Command

13. ABSTRACT

The dynamic response of pressure transmission lines to pulse input was investigated experimentally. The most commonly used commercially available flexible Tygon tubings were examined at a constant 1/2-psi air pressure with a frequency up to 300 cps. Short tubings, from 1 inch to 3 feet and inside diameters between .052 inch and 1/4 inch, were tested in the experiment. Pressure transducers were selected which had very small internal volume and the reference transducer was kept at a practical minimum distance from the pressure source. Tubing with and without inlet restriction has been investigated to determine the phenomenon of resonant frequency. To determine the effect of the elastic wall of the tubing on the pressure response, comparison measurements were taken in rigid wall, flexible Tygon, and rubber tubings. Phase shift of flexible tubings with various lengths and inside diameters were determined for the frequency range 0-300 cps.

DD FORM 1 JAN 64 1473

14. KEY WORDS	LINK A		LINK B		LINK C	
	ROLE	WT	ROLE	WT	ROLE	WT
Pressure measurement Dynamic response Instrumentation Fluid mechanics Turbulent pressure fluctuations						

INSTRUCTIONS

1. ORIGINATING ACTIVITY: Enter the name and address of the contractor, subcontractor, grantee, Department of Defense activity or other organization *(corporate author)* issuing the report.

2*a*. REPORT SECURITY CLASSIFICATION: Enter the overall security classification of the report. Indicate whether "Restricted Data" is included. Marking is to be in accordance with appropriate security regulations.

2*b*. GROUP: Automatic downgrading is specified in DoD Directive 5200.10 and Armed Forces Industrial Manual. Enter the group number. Also, when applicable, show that optional markings have been used for Group 3 and Group 4 as authorized.

3. REPORT TITLE: Enter the complete report title in all capital letters. Titles in all cases should be unclassified. If a meaningful title cannot be selected without classification, show title classification in all capitals in parenthesis immediately following the title.

4. DESCRIPTIVE NOTES: If appropriate, enter the type of report, e.g., interim, progress, summary, annual, or final. Give the inclusive dates when a specific reporting period is covered.

5. AUTHOR(S): Enter the name(s) of author(s) as shown on or in the report. Enter last name, first name, middle initial. If military, show rank and branch of service. The name of the principal author is an absolute minimum requirement.

6. REPORT DATE: Enter the date of the report as day, month, year; or month, year. If more than one date appears on the report, use date of publication.

7*a*. TOTAL NUMBER OF PAGES: The total page count should follow normal pagination procedures, i.e., enter the number of pages containing information.

7*b*. NUMBER OF REFERENCES: Enter the total number of references cited in the report.

8*a*. CONTRACT OR GRANT NUMBER: If appropriate, enter the applicable number of the contract or grant under which the report was written.

8*b*, 8*c*, & 8*d*. PROJECT NUMBER: Enter the appropriate military department identification, such as project number, subproject number, system numbers, task number, etc.

9*a*. ORIGINATOR'S REPORT NUMBER(S): Enter the official report number by which the document will be identified and controlled by the originating activity. This number must be unique to this report.

9*b*. OTHER REPORT NUMBER(S): If the report has been assigned any other report numbers *(either by the originator or by the sponsor)*, also enter this number(s).

10. AVAILABILITY/LIMITATION NOTICES: Enter any limitations on further dissemination of the report, other than those imposed by security classification, using standard statements such as:

(1) "Qualified requesters may obtain copies of this report from DDC."

(2) "Foreign announcement and dissemination of this report by DDC is not authorized."

(3) "U. S. Government agencies may obtain copies of this report directly from DDC. Other qualified DDC users shall request through _____."

(4) "U. S. military agencies may obtain copies of this report directly from DDC. Other qualified users shall request through _____."

(5) "All distribution of this report is controlled. Qualified DDC users shall request through _____."

If the report has been furnished to the Office of Technical Services, Department of Commerce, for sale to the public, indicate this fact and enter the price, if known.

11. SUPPLEMENTARY NOTES: Use for additional explanatory notes.

12. SPONSORING MILITARY ACTIVITY: Enter the name of the departmental project office or laboratory sponsoring *(paying for)* the research and development. Include address.

13. ABSTRACT: Enter an abstract giving a brief and factual summary of the document indicative of the report, even though it may also appear elsewhere in the body of the technical report. If additional space is required, a continuation sheet shall be attached.

It is highly desirable that the abstract of classified reports be unclassified. Each paragraph of the abstract shall end with an indication of the military security classification of the information in the paragraph, represented as *(TS)*, *(S)*, *(C)*, *or (U)*.

There is no limitation on the length of the abstract. However, the suggested length is from 150 to 225 words.

14. KEY WORDS: Key words are technically meaningful terms or short phrases that characterize a report and may be used as index entries for cataloging the report. Key words must be selected so that no security classification is required. Identifiers, such as equipment model designation, trade name, military project code name, geographic location, may be used as key words but will be followed by an indication of technical context. The assignment of links, rules, and weights is optional.

MINIMUM BASIC DISTRIBUTION LIST FOR USAMC SCIENTIFIC AND TECHNICAL REPORTS IN METEOROLOGY AND ATMOSPHERIC SCIENCES

Commanding General (1)
U. S. Army Materiel Command
Attn: AMCRD-RV-A
Washington, D. C. 20315

Commanding General (1)
U. S. Army Electronics Command
Attn: AMSEL-EW
Fort Monmouth, New Jersey 07703

Commanding General (1)
U. S. Army Test and Evaluation Command
Attn: NBC Directorate
Aberdeen Proving Ground, Maryland 21005

Commanding Officer (1)
U. S. Army Ballistics Research Laboratories
Attn: AMXBR-IA
Aberdeen Proving Ground, Maryland 21005

Chief, Atmospheric Physics Division (2)
Atmospheric Sciences Laboratory
U. S. Army Electronics Command
Fort Monmouth, New Jersey 07703

U. S. Army Munitions Command (1)
Attn: Irving Solomon
Operations Research Group
Edgewood Arsenal, Maryland 21010

Commanding Officer (1)
U. S. Army Dugway Proving Ground
Attn: Meteorology Division
Dugway, Utah 84022

Commanding Officer (1)
U. S. Army CDC, CBR Agency
Attn: Mr. N. W. Bush
Fort McClellan, Alabama 36205

Commanding General (1)
U. S. Army Test and Evaluation Command
Attn: AMSTE-EL
Aberdeen Proving Ground, Maryland 21005

Commandant (1)
U. S. Army Signal School
Attn: Meteorological Department
Fort Monmouth, New Jersey 07703

Assistant Chief of Staff for Force Development (1)
CBR Nuclear Operations Directorate
Department of the Army
Washington, D. C. 20310

Director (1)
Atmospheric Sciences Programs
National Sciences Foundation
Washington, D. C. 20550

Assistant Secretary of Defense (1)
Research and Engineering
Attn: Technical Library
Washington, D. C. 20301

R. A. Taft Sanitary Engineering Center (1)
Public Health Service
4676 Columbia Parkway
Cincinnati, Ohio

Dr. Hans A. Panofsky (1)
Department of Meteorology
The Pennsylvania State University
University Park, Pennsylvania

Commanding General (1)
U. S. Continental Army Command
Attn: Reconnaissance Branch ODCS
for Intelligence
Fort Monroe, Virginia 23351

Commander (1)
Air Force Cambridge Research Laboratories
Attn: CRZW
1065 Main Street
Waltham, Massachusetts

President (1)
U. S. Army Artillery Board
Fort Sill, Oklahoma 73504

National Center for Atmospheric Research (1)
Attn: Library
Boulder, Colorado

Dr. J. E. Cermak, Head (15)
Fluid Mechanics Program
Colorado State University
Fort Collins, Colorado 80521

Author (1)

Chief of Research and Development (1)
Department of the Army
Attn: CRD/M
Washington, D. C. 20310

Commanding General (1)
U. S. Army Missile Command
Attn: AMSMI-RRA
Redstone Arsenal, Alabama 35809

Commanding General (1)
U. S. Army Natick Laboratories
Attn: Earth Sciences Division
Natick, Massachusetts 01762

Director, U. S. Army Engineer (1)
Waterways Experiment Station
Attn: WES-FV
Vicksburg, Mississippi 39181

Chief, Atmospheric Sciences Research Division (5)
Atmospheric Sciences Laboratory
U. S. Army Electronics Command
Fort Huachuca, Arizona 85613

Commanding Officer (1)
U. S. Army Frankford Arsenal
Attn: SMUFA-1140
Philadelphia, Pennsylvania 19137

Commandant (1)
U. S. Army Artillery and Missile School
Attn: Target Acquisition Department
Fort Sill, Oklahoma 73504

Commanding General (1)
U. S. Army Electronics Proving Ground
Attn: Field Test Department
Fort Huachuca, Arizona 85613

Commanding General (1)
U. S. Army Test and Evaluation Command
Attn: AMSTE-BAF
Aberdeen Proving Ground, Maryland 21005

Office of Chief Communications - Electronics (1)
Department of the Army
Attn: Electronics Systems Directorate
Washington, D. C. 20315

Chief of Naval Operations (1)
Department of the Navy
Attn: Code 427
Washington, D. C. 20350

Director (1)
Bureau of Research and Development
Federal Aviation Agency
Washington, D. C. 20553

Director of Meteorological Systems (1)
Office of Applications (FM)
National Aeronautics and Space Administration
Washington, D. C. 20546

Director (1)
Atmospheric Physics and Chemistry Laboratory
Environmental Science Services Administration
Boulder, Colorado

Andrew Morse (1)
Army Aeronautical Activity
Ames Research Center
Moffett Field, California 94035

Commanding Officer (2)
U. S. Army Cold Regions Research and
Engineering Laboratories
Attn: Environmental Research Branch
Hanover, New Hampshire 03755

Mr. Ned L. Kragness (1)
U. S. Army Aviation Materiel Command
SMOSM-E
12th and Spruce Streets
Saint Louis, Missouri 63166

Commanding Officer, U. S. Army (1)
Artillery Combat Development Agency
Fort Sill, Oklahoma 73504

Commander, USAR Air Weather Service (MATS) (1)
Attn: AWSSS/TIPD
Scott Air Force Base, Illinois

Dr. John Bogusky (1)
7310 Cedardale Drive
Alexandria, Virginia 22308

Commanding General (1)
U. S. Army Combat Development Command
Attn: CDCMR-E
Fort Belvoir, Virginia 22060

Commanding General (1)
U. S. Army Munitions Command
Attn: AMSMU-RE-R
Dover, New Jersey 07801

Commanding Officer (1)
U. S. Army Ballistics Research Laboratories
Attn: AMXBR-B
Aberdeen Proving Ground, Maryland 21005

Director (2)
Atmospheric Sciences Laboratory
U. S. Army Electronics Command
Fort Monmouth, New Jersey 07703

Chief, Atmospheric Sciences Office (2)
Atmospheric Sciences Laboratory
U. S. Army Electronics Command
White Sands Missile Range, New Mexico 88002

Commanding Officer (1)
U. S. Army Picatinny Arsenal
Attn: SMUPA-TV-3
Dover, New Jersey 07801

Commanding Officer (1)
U. S. Army Communications - Electronics
Combat Development Agency
Fort Monmouth, New Jersey 07703

Commanding General (1)
Deseret Test Center
Attn: Design and Analysis Division
Fort Douglas, Utah 84113

Commandant (1)
U. S. Army CBR School Micrometeorological
Section
Fort McClellan, Alabama 36205

Assistant Chief of Staff for Intelligence (1)
Department of the Army
Attn: ACSI-DERSI
Washington, D. C. 20310

Officer in Charge (1)
U. S. Naval Weather Research Facility
U. S. Naval Air Station, Building 4-28
Norfolk, Virginia 23500

Chief, Fallout Studies Branch (1)
Division of Biology and Medicine
Atomic Energy Commission
Washington, D. C. 20545

Director (1)
U. S. Weather Bureau
Attn: Librarian
Washington, D. C. 20235

Dr. Albert Miller (1)
Department of Meteorology
San Jose State College
San Jose, California 95114

Mrs. Francis L. Wheedon (1)
Army Research Office
3045 Columbia Pike
Arlington, Virginia 22201

Commander (1)
Air Force Cambridge Research Laboratories
Attn: CRXL
L. G. Hanscom Field
Bedford, Massachusetts

Harry Moses, Asso. Meteorologist (1)
Radiological Physics Division
Argonne National Laboratory
9700 S. Cass Avenue
Argonne, Illinois 60440

Defense Documentation Center (20)
Cameron Station
Alexandria, Virginia 22314

Office of U. S. Naval Weather Service (1)
U. S. Naval Air Station
Washington, D. C. 20390

Dr. Gerald Gill (1)
University of Michigan
Ann Arbor, Michigan 48103